Molecular Cell 24, 977–984, December 28, 2006 ©2006 Elsevier Inc. DOI 10.1016/j.molcel.2006.11.015

Cooperation of Multiple Chaperones Required for the Assembly of Mammalian 20S Proteasomes

Short Article

Yuko Hirano,[1] Hidemi Hayashi,[2,4] Shun-ichiro Iemura,[5] Klavs B. Hendil,[6] Shin-ichiro Niwa,[4] Toshihiko Kishimoto,[2,3] Masanori Kasahara,[7] Tohru Natsume,[5] Keiji Tanaka,[1] and Shigeo Murata[1,8,*]

[1] Laboratory of Frontier Science
Core Technology and Research Center
Tokyo Metropolitan Institute of Medical Science
Bunkyo-ku, Tokyo 113-8613
[2] Proteome Analysis Center
[3] Department of Biomolecular Science
Faculty of Science
Toho University
Funabashi, Chiba 274-8510
[4] Link Genomics, Inc.
Chuo-ku, Tokyo 103-0024
[5] National Institute of Advanced Industrial Science and Technology
Biological Information Research Center
Kohtoh-ku, Tokyo 135-0064
Japan
[6] Institute of Molecular Biology and Physiology
University of Copenhagen
13 Universitetsparken
DK 2100 Copenhagen
Denmark
[7] Department of Pathology
Hokkaido University Graduate School of Medicine
Sapporo, Hokkaido 060-8638
[8] PRESTO
Japan Science and Technology Agency
Kawaguchi, Saitama 332-0012
Japan

Summary

The 20S proteasome is a catalytic core of the 26S proteasome, a central enzyme in the degradation of ubiquitin-conjugated proteins. It is composed of 14 distinct gene products that form four stacked rings of seven subunits each, $\alpha_{1-7}\beta_{1-7}\beta_{1-7}\alpha_{1-7}$. It is reported that the biogenesis of mammalian 20S proteasomes is assisted by proteasome-specific chaperones, named PAC1, PAC2, and hUmp1, but the details are still unknown. Here, we report the identification of a chaperone, designated PAC3, as a component of α rings. Although it can intrinsically bind directly to both α and β subunits, PAC3 dissociates before the formation of half-proteasomes, a process coupled with the recruitment of β subunits and hUmp1. Knockdown of PAC3 impaired α ring formation. Further, PAC1/2/3 triple knockdown resulted in the accumulation of disorganized half-proteasomes that are incompetent for dimerization. Our results describe a cooperative system of multiple chaperones involved in the correct assembly of mammalian 20S proteasomes.

*Correspondence: smurata@rinshoken.or.jp

Introduction

The ubiquitin-proteasome system is the main nonlysosomal route for intracellular protein degradation in eukaryotes. Short-lived proteins as well as abnormal proteins are recognized by the ubiquitin system and are marked with ubiquitin chains as degradation signals. Polyubiquitinated proteins are then recognized and degraded by 26S proteasomes. The 26S proteasome is composed of one proteolytically active 20S proteasome and two 19S regulatory particles, each attached to one end of the 20S proteasome. The 20S proteasome is a barrel-shaped complex made of two outer α rings and two inner β rings that is a conserved architecture in eukaryotes (Groll et al., 1997, 2005; Unno et al., 2002). The α and β rings are each made up of seven structurally similar subunits, of the α or β type, respectively. The proteolytic activity is exerted by three of the β subunits, namely β1, β2, and β5, which are synthesized in an inactive precursor form and whose propeptides are removed to allow the formation of active sites, accompanied by the assembly of 20S proteasomes.

Our previous work indicated that the assembly of mammalian 20S proteasomes is an ordered multistep process, starting from α ring formation with the help of proteasome-specific chaperones named PAC1 (proteasome assembling chaperone 1) and PAC2 (Hirano et al., 2005). The PAC1-PAC2 heterodimer binds to early α subunit assembly intermediates that contain a restricted subset of α subunits and promotes the formation of heteroheptameric α rings. Moreover, PAC1-PAC2 is responsible for suppressing the formation of off-pathway, nonproductive α ring dimers and thus is important for efficient half-proteasome formation (Hirano et al., 2005). Mammalian half-proteasomes are composed of seven α subunits, seven β subunits, some of which are in precursor forms, and proteasome-dedicated chaperones such as hUmp1 (POMP, Proteassemblin, a homolog of yeast Ump1) (Burri et al., 2000; Griffin et al., 2000; Ramos et al., 1998; Witt et al., 2000) and PAC1-PAC2 (Hirano et al., 2005). Lastly, dimerization of the two half-proteasomes occurs with the help of hUmp1, which completes the maturation of 20S proteasomes, with removal of propeptides of β subunits followed by degradation of hUmp1 and the PAC1-PAC2 heterodimer (Chen and Hochstrasser, 1996; De et al., 2003; Heinemeyer et al., 2004; Hirano et al., 2005; Kingsbury et al., 2000; Nandi et al., 1997; Ramos et al., 1998; Schmidtke et al., 1996). However, the mechanism responsible for half-proteasome formation after the assembly of α rings, i.e., how β subunits and hUmp1 are assembled on α rings, remains elusive. We speculated that another chaperone might be involved in this step.

Results and Discussion

Identification of PAC3 as a Component of α Rings

To identify molecules that are potentially involved in 20S proteasome maturation, we purified α rings from HEK293T cells stably expressing Flag-PAC1 and analyzed them

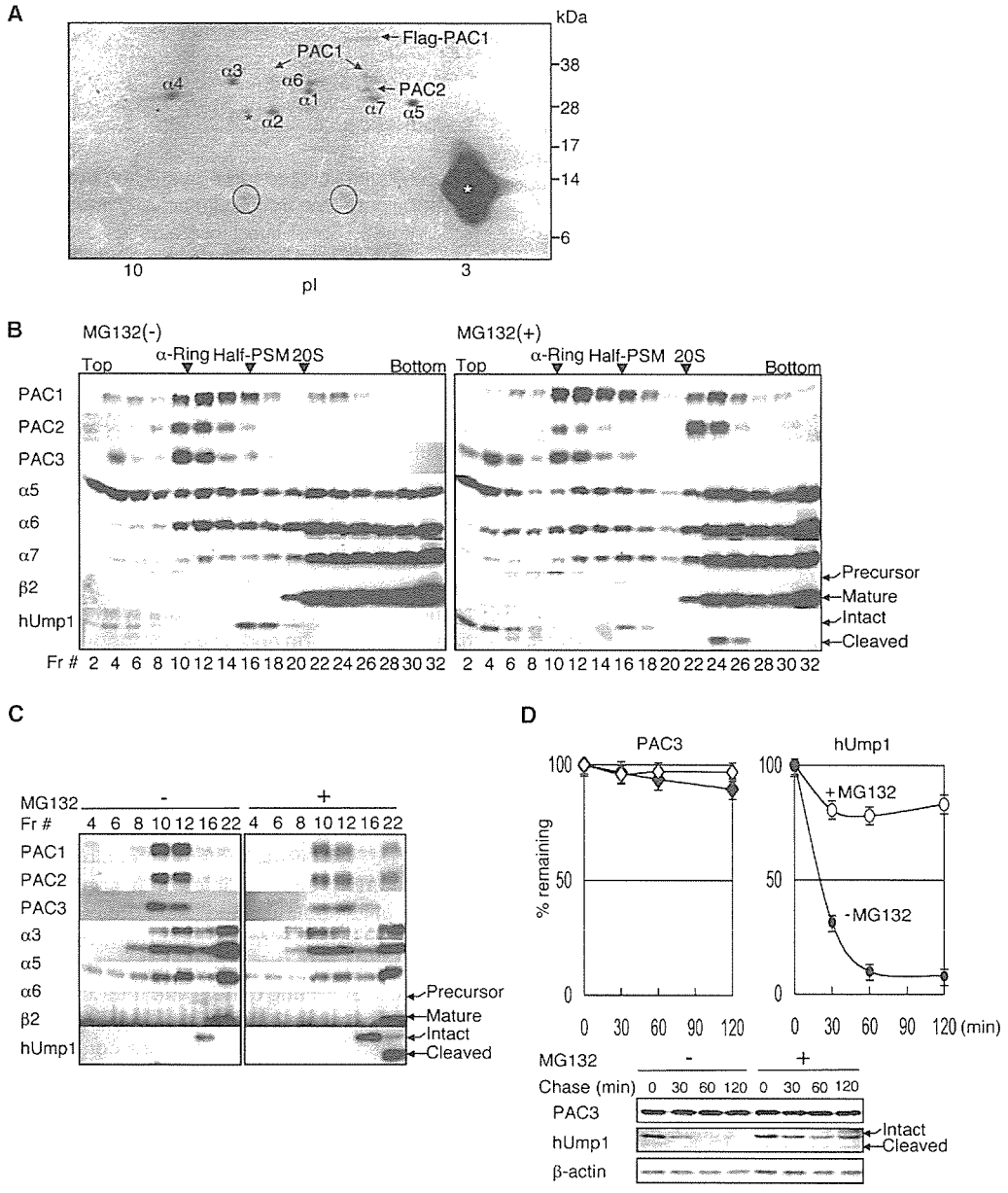

Figure 1. Identification of PAC3 as a Component of α Rings

(A) 2D-PAGE and CBB staining of purified α rings. The α rings were purified from HEK293T cells stably expressing Flag-PAC1 by glycerol gradient centrifugation followed by immunoprecipitation of α ring fractions with M2 agarose. All the spots were identified by MS/MS. The two spots indicated by circles represent hypothetical protein MGC10911. Asterisks indicate nonspecific spots.

(B) 4%–24% glycerol gradient centrifugation of the extracts of HEK293T cells treated with or without MG132. Fractions were immunoblotted as indicated. Arrowheads depict the locations of subcomplexes of proteasomes. Half-PSM, half-proteasomes; 20S, 20S proteasomes. Note that 26S proteasomes sediment near the bottom fraction.

(C) Fractions from (B) were immunoprecipitated with anti-α6 antibody, followed by immunoblotting.

(D) The half-life of PAC3 and hUmp1. Cycloheximide was added to HEK293T cells pretreated with or without 20 μM MG132 for 20 min, and the cells were chased for the indicated time points in the presence or absence of MG132, respectively. The cell lysates were subjected to immunoblotting for PAC3, hUmp1, and β-actin (loading control, bottom). The decay curves of PAC3 (top, left) and hUmp1 (top, right) were generated from the band quantification of the bottom panels. Data are mean ± SEM values of three independent experiments.

by two-dimensional polyacrylamide gel electrophoresis (2D-PAGE). In addition to the spots of α subunits and PAC1-PAC2 heterodimer, we found two spots of ~14 kDa. Using tandem mass spectrometry (MS/MS), we identified the two spots as a protein called MGC10911 (Figure 1A). We renamed it PAC3 (for proteasome assembling chaperone-3). PAC3 is a small protein of 122 amino acids with no distinct domains or homology to any other known proteins, and its function was entirely unknown. We found genes with significant similarity in metazoans, plants, and fungi, as for PAC2, PAC3, and hUmp1, but in metazoans and fungi as for PAC1 (Figure S1 in the Supplemental Data available with this article online).

First, to examine the behavior of endogenous PAC3, extracts from HEK293T cells were separated by glycerol

gradient centrifugation. PAC3 was located in the α ring fractions (fractions 10–12), i.e., in fractions without β subunits but with α subunits and PAC1-PAC2 (Figure 1B, left). The association of PAC3 with α subunits and PAC1-PAC2 was confirmed by immunoprecipitation with anti-α6 antibody followed by immunoblotting, indicating that PAC3 is a component of α rings, similar to PAC1-PAC2 (Figure 1C, left). Interestingly, when the cells were treated with a proteasome inhibitor, MG132, PAC3 was increased in the light fractions (fractions 2–6), whereas PAC1-PAC2 accumulated in the 20S proteasome fractions (fractions 22–24) as reported previously by our group (Figure 1B, right panels) (Hirano et al., 2005). This suggests that PAC3 dissociates from precursor proteasomes during the maturation pathway, unlike PAC1-PAC2 and hUmp1 (Hirano et al., 2005; Ramos et al., 1998). The increase in PAC3 in the light fractions does not represent an increase in newly synthesized PAC3 upon MG132 treatment, because PAC3 messenger RNA was not increased at this point of time (data not shown). To examine whether the stability of PAC3 is also regulated differently from that of PAC1-PAC2 and hUmp1, which have been shown to be short-lived proteins (Hirano et al., 2005; Ramos et al., 1998), we measured the half-life of PAC3 as well as that of hUmp1 by determining the protein levels at various time points after treatment with cycloheximide. As shown in Figure 1D, hUmp1 had a short half-life of about 20 min, which was greatly prolonged by MG132. This observation is consistent with the previous report (Ramos et al., 1998). As for hUmp1, we noted accumulation of its free forms (Figure 1B, right, fractions 2–6) as well as its cleaved forms in 20S proteasome fractions upon MG132 treatment (Figures 1B–1D). In contrast, PAC3 had a much longer half-life, which was not affected by MG132. These results suggest that PAC3 is involved in the maturation of 20S proteasomes and behaves differently from PAC1-PAC2 and hUmp1.

Knockdown of PAC3 Attenuates α Ring Formation

To elucidate the role of PAC3 in the assembly of the 20S proteasome in vivo, we performed small interfering RNA (siRNA)-mediated knockdown of PAC3 as well as PAC1+PAC2 (PAC1/2), PAC1+PAC2+PAC3 (PAC1/2/3), and hUmp1 to specify their distinct roles. In PAC3 knockdown cells, where we achieved a 75% reduction of PAC3 mRNA (data not shown), polyubiquitin-conjugated proteins accumulated to a level comparable to that in PAC1/2 knockdown cells (Figure 2A). In PAC1/2/3 knockdown cells, the accumulation of polyubiquitinated proteins was enhanced, and the effect of such knockdown was as large as with hUmp1 knockdown (Figure 2A). Consistent with these observations, the decrease in chymotrypsin-like activity of proteasomes was comparable between PAC3 and PAC1/2 knockdown, and the activity was profoundly reduced in PAC1/2/3 knockdown, similar to that in hUmp1 knockdown. These results suggest that PAC1-PAC2 and PAC3 are not epistatic with each other but rather work differently or compensate each other.

To determine the role of PAC3 in the assembly of 20S proteasomes, extracts of knockdown cells were subjected to glycerol gradient analysis (Figure 2C and Figure S2). To compare the quantity of relevant components in each fraction, fractions corresponding to α ring, half-proteasome, and 20S proteasomes in each knockdown experiment were electrophoresed in the same gel (Figure 2D). PAC1/2 knockdown resulted in reduction of α ring peak and emergence of α ring dimers in the half-proteasome fractions (fractions 14–16) as we reported previously (Hirano et al., 2005), and it turned out that PAC3 was a component of this abnormal structure (Figure 2C, bottom left, and Figure 2D, lane 7), indicating that PAC3 plays no role in inhibiting the formation of α ring dimers. The accumulation of PAC3 in light fractions (Figure 2C, bottom left, fractions 4–6) was probably due to ineffective α ring formation in PAC1/2 knockdown cells. Ectopic expression of PAC3 in PAC1/2 knockdown cells did not complement the phenotypes in regard to the formation of α ring dimers and reduction in proteasome activity (Figure S3), indicating that PAC3 and PAC1-PAC2 play distinct roles in α ring formation and do not function redundantly.

In PAC3 knockdown cells, we also observed a reduction of the α ring peak, but no α ring dimers (Figure 2C, top right). Consequently, half-proteasomes, which included α subunits, pro-β subunits, and hUmp1 in proportions like those observed in control cells, were formed to a lesser extent, resulting in decreased formation of 20S proteasomes (Figure 2D, lanes 8 and 13). In addition, PAC1-PAC2 accumulated in light fractions, and free forms of α subunits were increased in PAC3 knockdown cells as well as PAC1/2 and PAC1/2/3 knockdown cells (Figure 2C, top right, and Figure S4). These results suggest that PAC3 plays an important role in α ring assembly and that poor α ring formation resulted in surplus PAC1-PAC2 heterodimer and free α subunits in light fractions.

Simultaneous Loss of PAC1-PAC2 and PAC3 Causes Accumulation of Disorganized Half-Proteasomes

Intriguingly, in PAC1/2/3 knockdown cells, several α subunits and β subunits, including pro-β2 and hUmp1, cosedimented in the half-proteasome fractions to levels comparable to, or even higher (for example, hUmp1, pro-β1, and pro-β2) than, those in control cells, but still the formation of 20S proteasomes was severely impaired (Figure 2C, bottom right, and Figure 2D, lanes 9 and 14). Specifically, the amount of pro-β5, whose propeptide is essential for 20S proteasome formation in yeast (Chen and Hochstrasser, 1996), was much smaller in the complex observed in the half-proteasome fraction of PAC1/2/3 knockdown cells than control cells (Figure 2D, lanes 6 and 9, and Figure 2E). Considering that α ring formation is attenuated by knockdown of both PAC1/2 and PAC3, these results suggest that this complex of abnormal half-proteasomes, observed in PAC1/2/3 knockdown cells, accumulated because it could not dimerize to form mature 20S proteasomes, at least due to a shortage of pro-β5, which should accompany a disorganized constitution of this abnormal half-proteasomes.

Taken together, the knockdown experiments suggest that both PAC1-PAC2 and PAC3 contribute to α ring formation by separate mechanisms, and thus, the effects of knockdowns are additive. In addition, our results suggest that PAC1-PAC2 and PAC3 act cooperatively on the correct formation of half-proteasomes. On the other hand, knockdown of hUmp1 did not influence

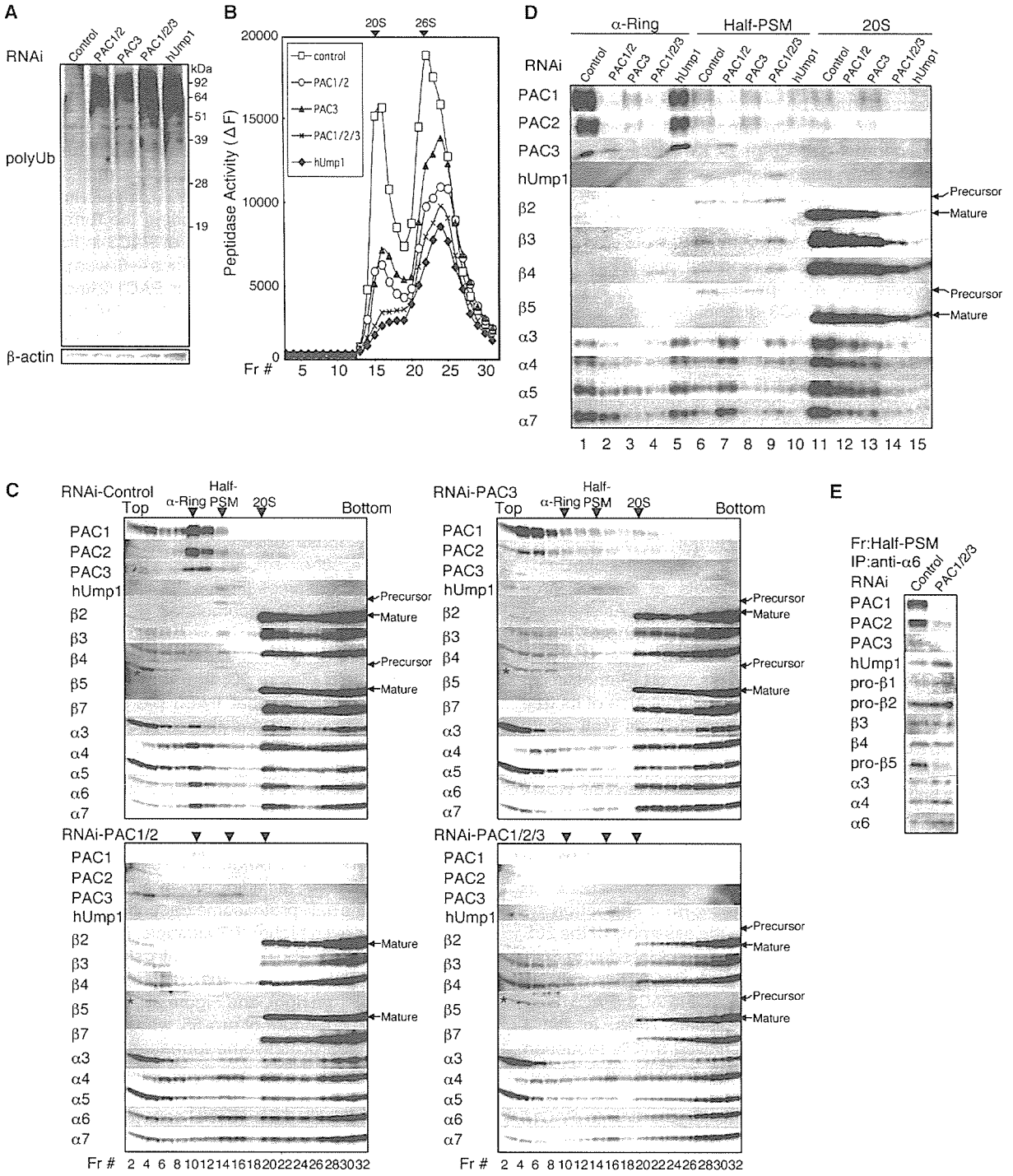

Figure 2. siRNA-Mediated Knockdown of PAC3 Causes Defect in Proteasome Assembly

siRNAs targeting PAC1/2, PAC3, PAC1/2/3, hUmp1, or control were transfected into HEK293T cells. The whole-cell extracts (A) and fractions separated by 8%–32% (B) or 4%–24% (C–E) glycerol gradient centrifugation were immunoblotted (A, C, D, and E) or assayed for Suc-LLVY-MCA hydrolyzing activity of proteasomes (B). In (D), the peak fractions of the indicated subcomplexes from (C) (α ring, fraction 12; Half-PSM, fraction 16; and 20S, fraction 22) were subjected to SDS-PAGE in the same gel to compare the quantity of subunits. (E) Fraction 16 of control or PAC1/2/3 knockdown cells from (C) was immunoprecipitated with anti-α6 antibody, followed by immunoblotting. Data are representative of four experiments.

the sedimentation pattern of PAC3 or PAC1-PAC2 (Figure S2), consistent with the notion that hUmp1 is involved in the last step of the assembly, i.e., dimerization of half-proteasomes, and not in α ring and half-proteasome formation (Hirano et al., 2005; Ramos et al., 1998).

PAC3 Directly Associates with Both α and β Subunits

To gain mechanistic insight into the action of PAC3 and the differences between PAC3 and PAC1-PAC2, we set up in vitro binding experiments. First, we examined direct interactions between PACs. PAC3 did not bind to

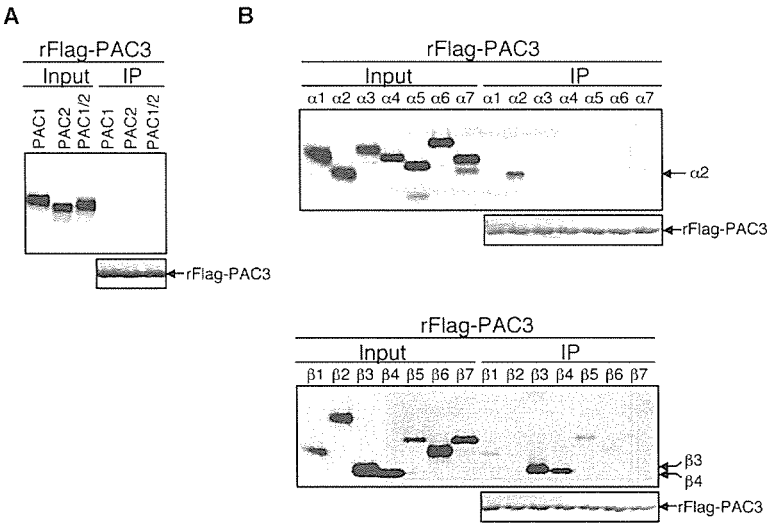

Figure 3. PAC3 Directly Binds to Both α2 and Several β Subunits

(A) Interactions of PAC3 with PAC1 and PAC2. Recombinant Flag-tagged PAC3 (rFlag-PAC3) was incubated with the indicated products translated and radiolabeled in reticulocyte lysates, immunoprecipitated with M2 agarose, and analyzed by SDS-PAGE and autoradiography.

(B) Interactions of PAC3 with individual α and β subunits. Interactions between rFlag-PAC3 and α or β subunits were analyzed as in (A).

PAC1 or PAC2 (Figure 3A). Next, we tested the interactions between PAC3 and each 20S proteasome subunit. PAC3 could directly bind to not only an α subunit (α2) but also to several β subunits, strongly to β3 and β4 but weakly to β1 and β5 (Figure 3B). This is in contrast to the property of PAC1-PAC2, which directly associated with α5 and α7, but not with any of the β subunits (Hirano et al., 2005). These results indicate that PAC1-PAC2 heterodimer and PAC3 are distinct entities that work at different aspects in the maturation of 20S proteasomes.

PAC3 Is Released from Precursor Proteasomes during Half-Proteasome Formation

Because PAC3 seemed to be released from precursor proteasomes during the maturation pathway (Figure 1B), we analyzed the precursor proteasomes that contain PAC3. An extract of HEK293T cells stably expressing Flag-PAC3, -hUmp1, or -PAC1 was separated by glycerol gradient centrifugation, and fractions 8–20, which included α rings (fraction 12) and half-proteasomes (fractions 16–18) were immunoprecipitated with anti-Flag antibody, followed by immunoblotting (Figure 4A). Flag-PAC3 did not precipitate hUmp1 or β subunits in half-proteasome fractions, and Flag-hUmp1 did not precipitate PAC3 at all (Figure 4A). Subsequently, we purified α rings and half-proteasomes from Flag-PAC2 and Flag-hUmp1 expressing cells, respectively, and subjected them to immunoblotting and CBB staining. Although half-proteasomes were loaded in much larger molar amounts, a band corresponding to PAC3, which was clearly visible in α rings, was not observed in half-proteasomes (Figure 4B and Figure S5). These results clearly show that the release of PAC3 from precursor proteasomes is coupled to the recruitment of hUmp1 and β subunits. Considering that PAC3 can directly bind to several β subunits in vitro (Figure 3B) and that PAC3 knockdown together with PAC1/2 knockdown resulted in production of disorganized half-proteasomes that were not competent for 20S proteasome formation (Figure 2), it is suggested that the association between PAC3 and β subunits is either intrinsically unstable in vivo or destabilized upon half-proteasome formation and that the release of PAC3 from precursor proteasomes is an obligatory step for the correct assembly of half-proteasomes by mediating interactions between α rings and β subunits.

Our present work provides a model (Figure 4C) where the chaperone PAC3 assists in the formation of α rings, together with PAC1-PAC2 heterodimer, and mediates correct formation of half-proteasomes in cooperation with PAC1-PAC2. PAC3 itself is then released and recycled in further rounds of proteasome assembly. The unique feature of PAC3 is its ability to interact with various β subunits, raising the possibility that it plays a role in the assembly of β subunits on α rings. In the present model, we emphasize that correct assembly of mammalian 20S proteasomes is achieved by the cooperative actions of multiple proteasome-specific chaperones.

Experimental Procedures

DNA Constructs

The cDNA encoding PAC3 was synthesized from total RNA isolated from HeLa cells using Superscript II (Invitrogen). PCR was carried out on the cDNA by using Phusion DNA polymerase (FINNZYMES). The cDNAs encoding PAC1, PAC2, PAC3, hUmp1, and proteasome α and β subunits were cloned into pcDNA3.1 (Invitrogen) and/or pIRESpuro3 (Clontech). All constructs were confirmed by sequencing. For expression of Flag-fusion protein, the cDNA was subcloned into pET22b (Novgen) in frame with a C-terminal Flag tag. For expression of GST and MBP-fusion proteins, the cDNAs were subcloned into pGEX6P-1 (Amersham) and pMAL (NEB), respectively.

Cell Culture

HEK293T cell lines were cultured in Dulbecco's modified Eagle's medium (Sigma), supplemented with 10% fetal calf serum (FCS), 100 IU/ml penicillin G, and 100 μg/ml streptomycin sulfate (all from Gibco-Invitrogen). Transfections of plasmids into HEK293T cells were performed with Fugene 6 (Roche). To generate stable cell lines, transfected HEK293T cells were selected with 5 μg/ml of puromycin. We used 20 μM MG132 (Peptide Institute) to inhibit proteasome activities for 2 hr before harvest. For cycloheximide-chase experiments, HEK293T cells were treated with 100 μg/ml cycloheximide (Sigma).

Protein Extracts, Immunological Analysis, and Antibodies

Cells were lysed in ice-cold lysis buffer (50 mM Tris-HCl [pH 7.5], 0.5% [v/v] NP-40, and 1 mM dithiothreitol [DTT]) with 2 mM ATP and 5 mM $MgCl_2$, and the extracts were clarified by centrifugation at 20,000 × g for 10 min at 4°C. The supernatants were mixed with

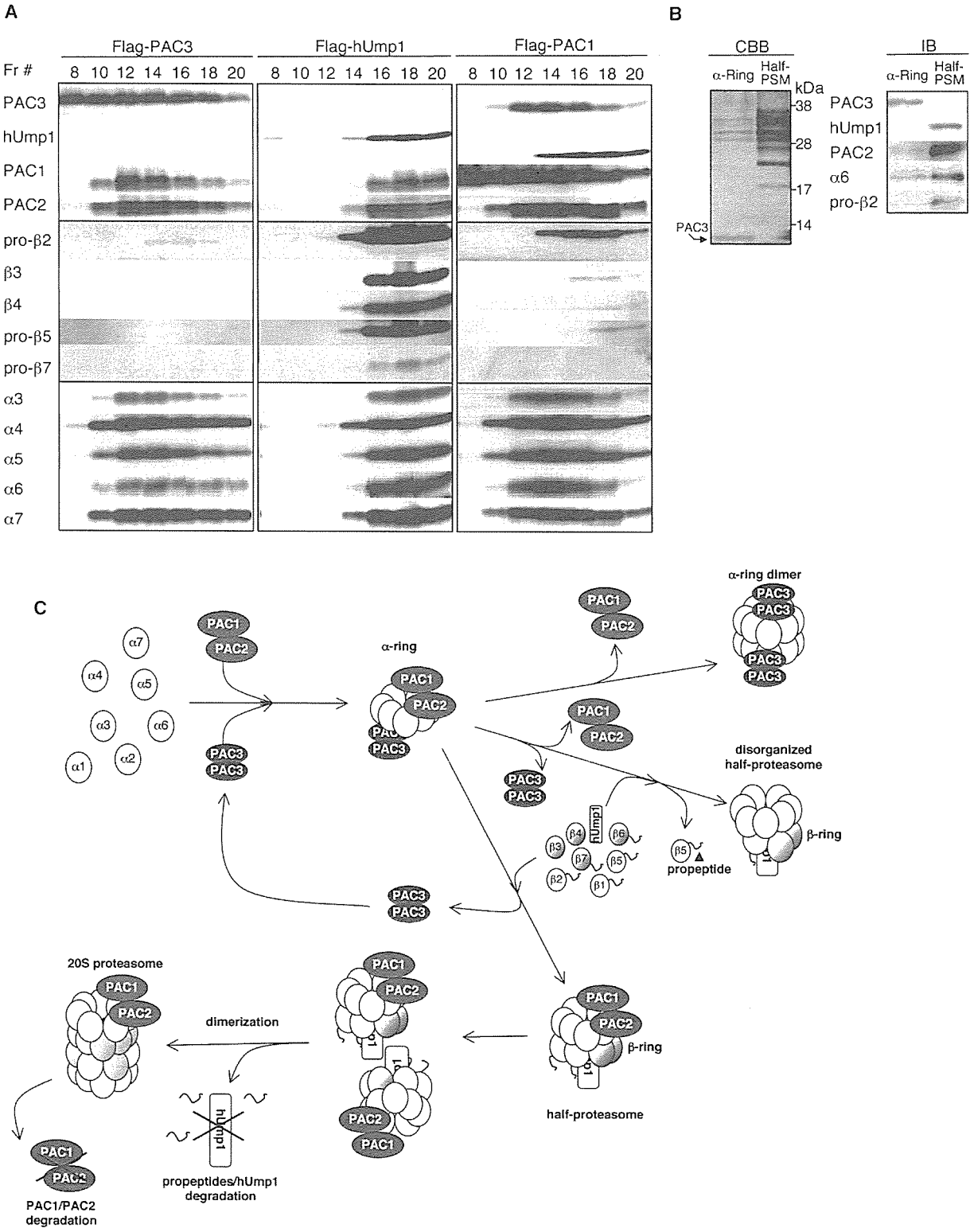

Figure 4. Mutually Exclusive Incorporation of PAC3 and hUmp1 into Precursor Proteasomes

(A) HEK293T cells stably expressing Flag-PAC3, -hUmp1, or -PAC1 were fractionated as in Figure 1B. The indicated fractions were immunoprecipitated with M2 agarose, resolved, and analyzed by SDS-PAGE and immunoblotting.

(B) SDS-PAGE followed by CBB staining (left) and immunoblotting (right) of purified α rings and half-proteasomes. α rings were purified from fraction 12 of Flag-PAC2 expressing cells. Half-proteasomes were purified from fraction 16 of Flag-hUmp1 expressing cells in (A). The band for PAC3 was identified by MS/MS. The 2D-PAGE analyses of these complexes are shown in Figure S5.

(C) A model for proteasome assembly assisted by multiple chaperones. PAC1-PAC2 heterodimer and PAC3, which probably forms homodimers based on the analysis of molecular sieve chromatography of the recombinant PAC3 (data not shown), assist α ring formation. Whereas PAC1-PAC2 suppresses off-pathway aggregation of α subunits and keeps α rings competent for half-proteasome formation, PAC3, which can bind

SDS sample buffer. SDS-PAGE (12% gel or 4%–12% gradient Bis-Tris gel [Invitrogen]) was performed according to the instructions provided by the manufacturer. The separated proteins were transferred onto polyvinylidene difluoride membrane and reacted with the indicated antibody. Development was performed with Western Lighting reagent (PerkinElmer). 2D-PAGE was performed as described previously (Murata et al., 2001).

For immunoprecipitation, we used antibodies MCP20 bound to protein G Sepharose (Amersham) in Figure 1C, antibodies MCP20 crosslinked to NHS-activated Sepharose (Amersham) in Figure 2E, or M2 Agarose (Sigma) in Figures 1A, 4A, and 4B. These beads were added to the extracts, mixed under constant rotation for 2 hr at 4°C, washed four times with lysis buffer with 30 mM NaCl, and boiled in SDS sample buffer. Otherwise, these washed samples were eluted with 100 μg/ml Flag peptides (Sigma) or with 0.2 M glycine-HCl (pH 2.8).

Anti-PAC1 and PAC2 polyclonal antibodies were described previously (Hirano et al., 2005). Anti-PAC3 polyclonal antibodies were raised in rabbits by using recombinant PAC3 (full-length) proteins, which were produced by cleavage of GST by PreScission protease (Amersham) after purification of GST-fused PAC3 proteins. Anti-hUmp1 polyclonal antibodies were raised in rabbits by using recombinant MBP-hUmp1 (full-length) proteins. Antibodies against proteasome α2 subunit (MCP21), α3 (MCP257), α4 (MCP34), α5 (MCP196), α6 (MCP20), α7 (MCP72), β1 (MCP421), β2 (MCP168), β3 (MCP102), and β7 (MCP205) were purchased from BioMol. Anti-β5 (P93250) and β4 (55F8) were prepared as described previously (Tanahashi et al., 2000). Anti-ubiquitin antibodies were obtained from Dako. Anti-β-actin antibodies were from Chemicon.

Glycerol Gradient Analysis

Cell extracts (1 mg of protein) were separated in 32 fractions by centrifugation (22 hr, 100,000 × g) in 4%–24% [v/v] or 8%–32% [v/v] linear gradients, as described previously (Hirano et al., 2005).

Binding Assay

In vitro labeling was performed by using TNT T7 Quick for PCR DNA system (Promega) with ^{35}S-labeled methionine, according to the procedure supplied by the manufacturer. Recombinant Flag-PAC3 proteins were expressed in *E. coli* and purified with M2 Agarose. Binding assay was performed in lysis buffer, and the resulting product was washed with lysis buffer with 150 mM NaCl before elution with Flag peptides. The eluates were separated by SDS-PAGE and visualized by autoradiography.

RNA Interference

siRNA targeting human PAC1, PAC2, PAC3, and hUmp1 with the following 19 nucleotide sequences were designed by B-Bridge and synthesized by Dharmacon. The targeting sequences of PAC1, PAC2, and hUmp1 were described previously (Hirano et al., 2005). These of PAC3 are 5′-CCGUGAAGGACAAAAGCAU-3′ and 5′-GAU CAAUUGUAGGAGGAAA-3′. Control siRNA (Non-specific Control Duplex VIII) was purchased from B-Bridge. Transfections of siRNAs into HEK293T cells were performed by using Lipofectamine 2000 at a final concentration of 50 nM. It was performed three times at intervals of 24 hr. The cells were analyzed 96 hr after first transfection.

Assay of Proteasome Activity

Peptidase activity was measured by using a fluorescent peptide substrate, succinyl-Leu-Leu-Val-Tyr-7-amido-4-methylcoumarin (Suc-LLVY-MCA), as described previously (Murata et al., 2001). Note that the assay was carried out in the presence of 0.03% SDS, which is a potent artificial activator of the latent 20S proteasome, as previously reported (Tanaka et al., 1989).

Supplemental Data

Supplemental Data include five figures and can be found with this article online at http://www.molecule.org/cgi/content/full/24/6/977/DC1/.

Acknowledgments

We thank K. Furuyama for technical support. This work was supported by grants from Japan Science and Technology Agency (to S.M.), the Ministry of Education, Science and Culture of Japan (to S.M. and K.T.), and NEDO (to T.N.). Y.H. was supported by Japan Society for the Promotion of Science.

Received: July 7, 2006
Revised: October 10, 2006
Accepted: November 15, 2006
Published: December 28, 2006

References

Burri, L., Hockendorff, J., Boehm, U., Klamp, T., Dohmen, R.J., and Levy, F. (2000). Identification and characterization of a mammalian protein interacting with 20S proteasome precursors. Proc. Natl. Acad. Sci. USA *97*, 10348–10353.

Chen, P., and Hochstrasser, M. (1996). Autocatalytic subunit processing couples active site formation in the 20S proteasome to completion of assembly. Cell *86*, 961–972.

De, M., Jayarapu, K., Elenich, L., Monaco, J.J., Colbert, R.A., and Griffin, T.A. (2003). β2 subunit propeptides influence cooperative proteasome assembly. J. Biol. Chem. *278*, 6153–6159.

Griffin, T.A., Slack, J.P., McCluskey, T.S., Monaco, J.J., and Colbert, R.A. (2000). Identification of proteassemblin, a mammalian homologue of the yeast protein, Ump1p, that is required for normal proteasome assembly. Mol. Cell Biol. Res. Commun. *3*, 212–217.

Groll, M., Ditzel, L., Lowe, J., Stock, D., Bochtler, M., Bartunik, H.D., and Huber, R. (1997). Structure of 20S proteasome from yeast at 2.4 Å resolution. Nature *386*, 463–471.

Groll, M., Bochtler, M., Brandstetter, H., Clausen, T., and Huber, R. (2005). Molecular machines for protein degradation. ChemBioChem *6*, 222–256.

Heinemeyer, W., Ramos, P.C., and Dohmen, R.J. (2004). The ultimate nanoscale mincer: assembly, structure and active sites of the 20S proteasome core. Cell. Mol. Life Sci. *61*, 1562–1578.

Hirano, Y., Hendil, K.B., Yashiroda, H., Iemura, S., Nagane, R., Hioki, Y., Natsume, T., Tanaka, K., and Murata, S. (2005). A heterodimeric complex that promotes the assembly of mammalian 20S proteasomes. Nature *437*, 1381–1385.

Kingsbury, D.J., Griffin, T.A., and Colbert, R.A. (2000). Novel propeptide function in 20 S proteasome assembly influences β subunit composition. J. Biol. Chem. *275*, 24156–24162.

Murata, S., Udono, H., Tanahashi, N., Hamada, N., Watanabe, K., Adachi, K., Yamano, T., Yui, K., Kobayashi, N., Kasahara, M., et al. (2001). Immunoproteasome assembly and antigen presentation in mice lacking both PA28α and PA28β. EMBO J. *20*, 5898–5907.

Nandi, D., Woodward, E., Ginsburg, D.B., and Monaco, J.J. (1997). Intermediates in the formation of mouse 20S proteasomes: implications for the assembly of precursor β subunits. EMBO J. *16*, 5363–5375.

Ramos, P.C., Hockendorff, J., Johnson, E.S., Varshavsky, A., and Dohmen, R.J. (1998). Ump1p is required for proper maturation of the 20S proteasome and becomes its substrate upon completion of the assembly. Cell *92*, 489–499.

Schmidtke, G., Kraft, R., Kostka, S., Henklein, P., Frommel, C., Lowe, J., Huber, R., Kloetzel, P.M., and Schmidt, M. (1996). Analysis of mammalian 20S proteasome biogenesis: the maturation of β-subunits is an ordered two-step mechanism involving autocatalysis. EMBO J. *15*, 6887–6898.

Tanahashi, N., Murakami, Y., Minami, Y., Shimbara, N., Hendil, K.B., and Tanaka, K. (2000). Hybrid proteasomes. Induction by interferon-γ and contribution to ATP-dependent proteolysis. J. Biol. Chem. *275*, 14336–14345.

directly to several β subunits, dissociates before the formation of half-proteasomes, a process coupled to the recruitment of β subunits and hUmp1. Loss of both PAC1-PAC2 and PAC3 before β subunit incorporation causes formation of disorganized half-proteasomes that lack pro-β5 almost completely. Released PAC3 is recycled. Two half-proteasomes dimerize with the help of hUmp1, and propeptides of β subunits (β1, β2, β5, β6, and β7) were cleaved. hUmp1 and PAC1-PAC2 are subsequently degraded by the newly formed active 20S proteasomes.

Tanaka, K., Yoshimura, T., and Ichihara, A. (1989). Role of substrate in reversible activation of proteasomes (multi-protease complexes) by sodium dodecyl sulfate. J. Biochem. (Tokyo) *106*, 495–500.

Unno, M., Mizushima, T., Morimoto, Y., Tomisugi, Y., Tanaka, K., Yasuoka, N., and Tsukihara, T. (2002). The structure of the mammalian 20S proteasome at 2.75 Å resolution. Structure *10*, 609–618.

Witt, E., Zantopf, D., Schmidt, M., Kraft, R., Kloetzel, P.M., and Kruger, E. (2000). Characterisation of the newly identified human Ump1 homologue POMP and analysis of LMP7(β5i) incorporation into 20 S proteasomes. J. Mol. Biol. *301*, 1–9.

Molecular Biology of the Cell
Vol. 18, 569–580, February 2007

The Assembly Pathway of the 19S Regulatory Particle of the Yeast 26S Proteasome[D]

Erika Isono,*† Kiyoshi Nishihara,*‡ Yasushi Saeki,*§ Hideki Yashiroda,‖ Naoko Kamata,* Liying Ge,*¶ Takashi Ueda,* Yoshiko Kikuchi,* Keiji Tanaka,‖ Akihiko Nakano,*# and Akio Toh-e*§

*Department of Biological Sciences, Graduate School of Science, University of Tokyo, Tokyo 113-0033, Japan; †Entwicklungsgenetik, ZMBP, University of Tübingen, D-72076 Tübingen, Germany; ‖Tokyo Metropolitan Institute of Medical Science, Tokyo 113-8613, Japan; and #RIKEN Discovery Research Institute, Saitama 351-0198, Japan

Submitted July 26, 2006; Revised November 13, 2006; Accepted November 20, 2006
Monitoring Editor: William Tansey

The 26S proteasome consists of the 20S proteasome (core particle) and the 19S regulatory particle made of the base and lid substructures, and it is mainly localized in the nucleus in yeast. To examine how and where this huge enzyme complex is assembled, we performed biochemical and microscopic characterization of proteasomes produced in two lid mutants, *rpn5-1* and *rpn7-3*, and a base mutant Δ*N rpn2*, of the yeast *Saccharomyces cerevisiae*. We found that, although lid formation was abolished in *rpn5-1* mutant cells at the restrictive temperature, an apparently intact base was produced and localized in the nucleus. In contrast, in Δ*N rpn2* cells, a free lid was formed and localized in the nucleus even at the restrictive temperature. These results indicate that the modules of the 26S proteasome, namely, the core particle, base, and lid, can be formed and imported into the nucleus independently of each other. Based on these observations, we propose a model for the assembly process of the yeast 26S proteasome.

INTRODUCTION

The ubiquitin–proteasome system (UPS) is essential for the degradation of short-lived regulatory proteins that are involved in cell cycle regulation, DNA repair, signal transduction, apoptosis, and metabolic regulation as well as for the elimination of damaged or misfolded proteins (Hershko and Ciechanover, 1998; Schwartz and Ciechanover, 1999). The 26S proteasome acts at the final step of this pathway by degrading poly-ubiquitinated substrates, thereby ensuring the irreversibility of this pathway.

The 26S proteasome is a huge multicatalytic complex consisting of >30 different components that are divided into those of the 20S core particle (CP) and the 19S regulatory particle (RP). The RP can be biochemically further divided into two substructures, the base and the lid. The base consists of six AAA-ATPase subunits, *r*egulatory *p*article *t*riple-A ATPase (Rpt)1p–Rpt6p, and three non-ATPase subunits, *r*egulatory *p*article *n*on-ATPase (Rpn)1p, Rpn2p, and Rpn13p, whereas the lid is made of nine non-ATPases, Rpn3p, Rpn5p–Rpn9p, Rpn11p, Rpn12p, and Sem1p (Rpn15p) (Glickman *et al.*, 1998b; Leggett *et al.*, 2002; Funakoshi *et al.*, 2004; Sone *et al.*, 2004). Rpn10p, a non-ATPase subunit that binds polyubiquitin (Ub) chains (van Nocker *et al.*, 1996; Saeki *et al.*, 2002; Elsasser *et al.*, 2004), has been suggested to exist in the interface between the base and the lid (Fu *et al.*, 2001).

Interestingly, the composition of the lid is surprisingly similar to that of the COP9/signalosome and the eIF3, from which Glickman *et al.* (1998a) proposed that these protein complexes have diverged from a common ancestor. Most of the components of these complexes share a common proteasome/COP9/Initiation factor (PCI) domain, thought to serve as a scaffold for protein–protein interaction (Hofmann and Bucher, 1998), or a catalytic MPN+ domain (Maytal-Kivity *et al.*, 2002). Rpn11p (Verma *et al.*, 2002; Yao and Cohen, 2002; Guterman and Glickman, 2004) and CSN5 (Cope *et al.*, 2002), which are MPN+ domain proteins of the lid and the COP9, respectively, are the only known components to possess enzymatic activity in these complexes.

It was shown by immunoelectron microscopy (Wilkinson *et al.*, 1998) and by fluorescence microscopy of green fluorescent protein (GFP)-tagged proteasomes (Enenkel *et al.*, 1999) that in yeast, 26S proteasomes were mainly localized in the nucleus, especially on the inner nuclear membrane. Based on genetic data, the involvement of importin α/β in

This article was published online ahead of print in *MBC in Press* (http://www.molbiolcell.org/cgi/doi/10.1091/mbc.E06-07-0635) on November 29, 2006.

[D] The online version of this article contains supplemental material at *MBC Online* (http://www.molbiolcell.org).

Present addresses: ‡ Graduate School of Frontier Sciences, University of Tokyo, Chiba 277-8561, Japan; § Tokyo Metropolitan Institute of Medical Sciences, Tokyo 113-8613, Japan; ¶ Graduate School of Frontier Sciences, University of Tokyo, Tokyo 108-8639, Japan.

Address correspondence to: Akio Toh-e (toh-e@rinshoken.or.jp).

Abbreviations used: CBB, Coomassie brilliant blue; CP, core particle; FRAP, fluorescence recovery after photobleaching; GFP, green fluorescent protein; MCA, methycoumaryl-7-amide; NLS, nuclear localization signal; PCI, proteasome/COP9/Initiation factor; mRFP, monomeric red fluorescent protein; RP, regulatory particle; Rpn, regulatory particle non-ATPase; Rpt, regulatory particle triple A ATPase; Suc-LLVY, succinyl-leucyl-leucyl-valyl-tyrosyl; Ub, ubiquitin; UFD, ubiquitin fusion degradation; UPS, ubiquitin–proteasome system.

Table 1. Yeast strains used in this study

Strain	Relevant genotype	Source
W303-1A	MATa *leu2 trp1 his3 ura3 ssd1 can1 ade2*	Our stock
W303-1B	MATα *leu2 trp1 his3 ura3 ssd1 can1 ade2*	Our stock
YEK5	MATa *rpn7::rpn7-3-URA3*	Isono *et al.* (2004)
YEK6	MATα *rpn7::rpn7-3-URA3*	Isono *et al.* (2004)
YEK29	YEK5 *rpn11::RPN11-3×FLAG-HIS3*	Isono *et al.* (2004)
YEK79	MATα *pre6::PRE6-GFP-TRP1*	This study
YEK100	MATa *rpn5::rpn5-1-TRP1*	This study
YEK101	MATα *rpn5::rpn5-1-TRP1*	This study
YEK115	MATa *rpn11::RPN11-YGFP-TRP1*	This study
YEK147	MATa *rpn1::RPN1-YGFP-LEU2*	This study
YEK209	YEK5 *rpn11::RPN11-YGFP-TRP1*	This study
YEK211	YEK5 *pre6::PRE6-YGFP-LEU2*	This study
YEK213	YEK6 *rpn1::RPN1-YGFP-LEU2*	This study
YEK221	MATα *rpn7::RPN7-3×FLAG-KanMX*	This study
YEK225	YEK100 *rpn7::RPN7-3×FLAG-KanMX*	This study
YEK234	YAT2433 *rpn1::RPN1-3×FLAG-HIS3*	This study
YEK235	YAT2433 *rpn1::RPN1-YGFP-LEU2*	This study
YEK236	YAT2433 *rpn11::RPN11-YGFP-TRP1*	This study
YEK246	YAT2433 *srp1::srp1-49-LEU2*	This study
YEK247	YAT2433 *srp1::srp1-49-LEU2 rpn7::RPN7-YGFP-URA3*	This study
YEK248	YAT2433 *srp1::srp1-49-LEU2 rpn1::RPN1-YGFP-URA3*	This study
YKN6	YEK100 *pre1::PRE1-3×FLAG-HIS3*	This study
YKN8	YEK100 *rpn1::RPN1-3×FLAG-HIS3*	This study
YKN16	YEK100 *rpn1::RPN1-YGFP-LEU2*	This study
YKN18	YEK101 *pre6::PRE6-YGFP-TRP1*	This study
YAT2433	MATα Δ*rpn2-TRP1* [Top2612]	This study
YAT3507	YAT2433 *rpn11::RPN11-3×FLAG-LEU2*	This study
YYS37	MATa *pre1::PRE1-3×FLAG-HIS3*	Saeki *et al.* (2002)
YYS39	MATa *rpn1::RPN1-3×FLAG-HIS3*	Saeki *et al.* (2002)
YYS40	MATa *rpn11::RPN11-3×FLAG-HIS3*	Saeki *et al.* (2002)

All strains are in the W303 background.

the nuclear import of the proteasomes was suggested (Tabb *et al.*, 2000), and it was shown that in the mutant of importin α *srp1-49*, seclusion of GFP-fused proteasome in the nucleus was no longer observed (Wendler *et al.*, 2004). A study in fission yeast has shown that Cut8 is responsible for retaining the proteasome within the nucleus (Tatebe and Yanagida, 2000; Takeda and Yanagida, 2005).

The process of proteasome assembly has been a topic for recent studies and interesting facts have been elucidated. The CP, which is a stack of four seven-membered rings, in the order of α7β7β7α7, is imported into the nucleus as an α7β7 "half" proteasome (Chen and Hochstrasser, 1996; Ramos *et al.*, 1998), and maturation is thought to take place in the nucleus (Fehlker *et al.*, 2003). Ump1p, which associates specifically with half-proteasomes, is suggested to function as an accelerator in this process (Ramos *et al.*, 1998). Blm10p (formerly registered as Blm3p) was reported to act as an inhibitor of premature dimerization of the half-proteasomes (Fehlker *et al.*, 2003), but it is also suggested to be a functional homologue of the mammalian PA200, activator of the CP (Schmidt *et al.*, 2005). Recently, a study in mammalian cells showed that PAC1 and PAC2 work during the first step of assembly of the α ring (Hirano *et al.*, 2005).

For the assembly of the RP, no external factors are known to date. In previous studies, we have shown that partially assembled lid subcomplexes made up of five (lid$^{rpn7\text{-}3}$: Rpn5p, Rpn6p, Rpn8p, Rpn9p, and Rpn11p) or four (lid$^{rpn6\text{-}1}$: Rpn5p, Rpn8p, Rpn9p, and Rpn11p) components accumulate in lid mutants (Isono *et al.*, 2004, 2005). Because Rpn5p, Rpn8p, Rpn9p, and Rpn11p were included in both subcomplexes, we proposed these to be the "core" of lid formation. In this study, based on the analysis of an *rpn5* mutant and an *rpn2* mutant, we show, for the first time, that the formation and nuclear import of both the lid and the base are separable processes and that Rpn5p is indeed one of the core components of the lid.

MATERIALS AND METHODS

Strains, Media, and Genetic Methods

Yeast strains used in this work are listed in Table 1, and plasmids used for cloning and subcloning various genes and their fragments are listed in Table 2. Cells were cultured in omission medium prepared by removing appropriate nutrient(s) from synthetic complete (SC) medium, rich medium (YPDAU) (Sherman *et al.*, 1986), or SR-U in which 2% glucose of SC was replaced with 2% raffinose and uracil was omitted. *Escherichia coli* strain DH5α (*supE44 ΔlacU169* [ϕ80lacZ Δ*M15*] *hsdR17 recA1 endA1 gyrA96 thi-1 relA1*) was used for construction and propagation of plasmids. Yeast transformations were performed as described previously (Burk *et al.*, 2000).

Isolation of Temperature-sensitive Mutants

Temperature-sensitive *rpn5* mutants were screened as described previously (Isono *et al.*, 2005). The *RPN5* gene was amplified using primers Rpn5 Mut1 (BglII) 5′-GGCCAAGATTGTAGATCTGCTAGC-3′ and Rpn5 Mut2 (NotI) 5′-GGAAGCGGCCGCAACCAGGCTTGAGTTAAC-3′ and cloned between the BamHI–NotI sites of the YIp vector pRS304. The resulting plasmid pNS101 was used as a template for polymerase chain reaction (PCR) mutagenesis.

Gel Filtration

Total proteins (5 mg) were resolved on a Superose 6 column (GE Healthcare, Little Chalfont, Buckinghamshire, United Kingdom) as described previously (Isono *et al.*, 2005). For the subsequent fractionation of Superose 6-fractionated samples, 450 μl of the separated samples were applied onto a Superdex 200 gel filtration column (GE Healthcare) connected to a fast-performance liquid

Table 2. Plasmids used in this study

Plasmid	Characteristics	Source
pRS304	*TRP1 Amp*^{r}	Sikorski and Hieter (1989)
pRS313	*HIS3 CEN Amp*^{r}	Sikorski and Hieter (1989)
Ub-A-lacZ	*GAL1p-Ub-A-lacZ URA3 Amp*^{r}	Bachmair *et al.* (1986)
Ub-R-LacZ	*GAL1p-Ub-R-lacZ URA3 Amp*^{r}	Bachmair *et al.* (1986)
Ub-P-lacZ	*GAL1p-Ub-P-lacZ URA3 Amp*^{r}	Bachmair *et al.* (1986)
pTS901CL	*5×HA CEN LEU2 Amp*^{r}	Sasaki *et al.* (2000)
pEK152	*RPN11-YGFP-TRP1 Amp*^{r}	This study
pEK165	*PRE6-YGFP-TRP1 Amp*^{r}	This study
pEK221	*RPN5(−400bp ORF∼+1kb ORF) HIS3 CEN Amp*^{r}	This study
pEK252	*RPN1-YGFP-LEU2 Amp*^{r}	This study
pEK285	*NUP53-mRFP-LEU2 CEN Amp*^{r}	This study
pEK291	*RPN7-YGFP-URA3 Amp*^{r}	This study
pEK296	*RPN1-YGFP-URA3 Amp*^{r}	This study
pEK297	*RPN3-YGFP-URA3 CEN Amp*^{r}	This study
pEK298	*RPN7-YGFP-URA3 CEN Amp*^{r}	This study
pEK299	*RPN12-YGFP-URA3 CEN Amp*^{r}	This study
pEK300	*RPN15-YGFP-URA3 CEN Amp*^{r}	This study
pNS101	*RPN5 TRP1 Amp*^{r}	This study
pNS202	*GST-RPN5 Amp*^{r}	This study
TOp2612	*ΔN rpn2 (+437∼+2838) HIS3 CEN Amp*^{r}	This study

chromatograph (GE Healthcare) at a flow rate of 0.5 ml/min, and 500-μl serial fractions were collected using a fraction collector FRAC-100 (GE Healthcare).

Microscopy

Cells harboring GFP- or monomeric red fluorescent protein (mRFP)-fused proteins were photographed by using a BX52 fluorescence microscope (Olympus, Tokyo, Japan) with a UPlanApo 100×/1.45 objective (Olympus) equipped with a confocal scanner unit CSU20 (Yokogawa Electric, Tokyo, Japan) and an EMCCD camera (Hamamatsu Photonics, Bridgewater, NJ). GFP and mRFP were excited using the 488- and 568-nm Ar/Kr laser lines with GFP and RFP filters (Semrock, Rochester, NY), respectively. DNA stained with Hoechst 33342 was photographed using a 405-nm laser line with a UV filter (Semrock). Images were obtained and processed using the IPLab software (Scanalytics, Fairfax, VA) and processed using Photoshop 7.0 (Adobe Systems, Mountain View, CA). For DNA staining, a final concentration of 20 μg/ml Hoechst 33342 (Sigma-Aldrich, St. Louis, MO) was added to the cell suspension and incubated for 10 min at either 25 or 37°C under a light shade.

Fluorescence Recovery after Photobleaching (FRAP)

Samples used for FRAP experiments were embedded in agarose in the following way with modifications of the methods described previously (Hoepfner *et al.*, 2000). First, 100 μl of 1.7% agarose (Takara, Kyoto, Japan) dissolved in filtrated SC media was dropped on a prewarmed holed glass slide (Toshinriko, Tokyo, Japan), and immediately covered with a coverslip (Matsunami Glass, Osaka, Japan). Excess agarose was removed, and the glass slide was cooled until the agarose was set. The coverslip was carefully removed, and 3 μl of freshly cultured cells was dropped on the agarose plane and covered with a new coverslip and sealed. FRAP experiments were performed using a confocal laser-scanning microscope LSM510 META (Carl Zeiss, Jena, Germany) with a Plan-APOCHROMAT 100×/1.4 objective (Carl Zeiss). GFP was excited using the 488-nm laser lines from an Ar ion laser and a GFP filter. Photobleaching was achieved by scanning the selected region with maximal output of the 488-nm laser, and the recovery of the fluorescent signal was observed at the indicated time points under the same recording conditions as at 0 min. The stage was kept at 37°C with a stage-heater MATS-525F (Tokai Hit, Shizuoka, Japan). Fluorescence intensity of the original data was quantified using the LSM510 software, and images were processed with Photoshop 7.0 (Adobe Systems).

Indirect Immunofluorescence Method

For fixation, 420 μl of 37% formaldehyde was added to 3 ml of logarithmically growing cell culture (OD_{600} = 0.8–1.0) and incubated for 30 min at the incubation temperature. Cells were centrifuged and resuspended in 500 μl of phosphate-buffered saline (PBS)-formaldehyde (PBS/formaldehyde, 10:1) and incubated for 30 min at room temperature. For spheroplasting, cells were incubated with 200 μl of PBS-zymolyase (20 μg of zymolyase 100T [Seikagaku America, Rockville, MD]/1 ml of PBS) for 20 min at 30°C. Cells were then incubated in 200 μl of PBS containing 0.5% Triton X-100 for 30 min at room temperature. After washing twice, cells were resuspended in 200 μl of 3% bovine serum albumin in PBS for blocking and incubated for 1 h at room temperature. Mouse monoclonal anti-FLAG M2 antibody (Sigma-Aldrich, St. Louis, MO; 1/200 dilution) or anti-Rpn5p (1/100 dilution) antibody was used as primary antibody. Alexa Fluor 488 goat anti-mouse IgG (Molecular Probes, 1/400 dilution) or Alexa Fluor 546 goat anti-rabbit IgG (1/400 dilution; Invitrogen, Carlsbad, CA) was used as a secondary antibody. DNA was stained with 0.5 μg/ml 4,6-diamidino-2-phenylindole (DAPI) (Sigma-Aldrich).

RESULTS

Isolation of the Temperature-sensitive rpn5-1 Mutant

In our previous study, we found that partially assembled lid subcomplexes accumulated in temperature-sensitive lid mutants. Five (Rpn5p, Rpn6p, Rpn8p, Rpn9p, and Rpn11p) or four (Rpn5p, Rpn8p, Rpn9p, and Rpn11p) out of the nine components of the lid formed a stable complex in lid mutants, *rpn7-3* (Isono *et al.*, 2004) and *rpn6-1/rpn6-2* (Isono *et al.*, 2005), respectively. From these results and the fact that *RPN9* is a nonessential gene, we hypothesized that Rpn5p, Rpn8p, and Rpn11p may play pivotal roles in producing the core of the lid. To examine this hypothesis, we first focused on the function of Rpn5p.

To start with, we generated a temperature-sensitive mutant allele of *RPN5* by PCR-based random mutagenesis (Cadwell and Joyce, 1992; Toh-e and Oguchi, 2000) and named it *rpn5-1*. The *rpn5-1* mutant grew normally at 25°C, but it stopped growth after 6–8 h at 37°C (data not shown). The growth defect of the *rpn5-1* mutant at 37°C was complemented by a single copy of the wild-type *RPN5* gene, proving that the temperature sensitivity is due to a mutation within the *RPN5* gene and that the *rpn5-1* mutation is not dominant (Figure 1A). Sequencing analysis revealed that the *rpn5-1* open reading frame (ORF) possessed three mutations (Figure 1B), of which I180L or R344G alone did not lead to temperature-sensitive growth when introduced into the wild-type background. The nucleotide substitution from G to A at the 1245th nucleotide, leading to a nonsense mutation at the 415th tryptophan was found to be responsible for the temperature sensitivity (data not shown). Amounts of Rpn5-1p along with other proteasomal components were not significantly changed during incubation at the restrictive temperature, whereas a slight mobility shift of Rpn5-1p was

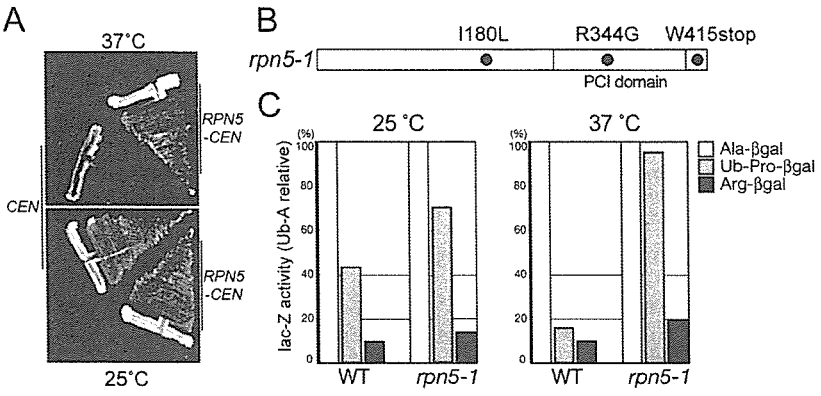

Figure 1. Characterization of the temperature-sensitive *rpn5* mutant. (A) *rpn5-1* (YEK100) cells carrying either a *CEN* vector (pRS314) or *RPN5-CEN* plasmid (pEK221) were streaked on YPDAU plates and photographed after incubating for 2 d at either 25 or 37°C. (B) Amino acid substitution in *rpn5-1*. The nucleotide sequence of the *rpn5-1* ORF was determined by the dideoxychain termination method and compared with that of the wild-type *RPN5* ORF. Gray, PCI domain. (C) Degradation of N-end rule pathway- and UFD pathway-substrates. Wild-type (W303-1A) and *rpn5-1* (YEK100) cells were transformed with plasmids expressing an N-end rule model substrate Ub-Ala-βgal or Ub-Arg-βgal, or a UFD pathway substrate Ub-Pro-βgal. Production of the model substrates was induced by adding 2% galactose to SR-U medium. Cells were harvested after 4 h of induction at either 25 or 37°C, and steady-state levels of β-galactosidase activity were assayed. The amounts of Ub-Pro-βgal and Arg-βgal are indicated relative to that of Ala-βgal. Average of three independent experiments is shown (open, Ala-βgal; light gray, Ub-Pro-βgal; and solid, Arg-βgal).

observed due to the C-terminal truncation (Supplemental Figure 1).

To examine the effect of the *rpn5-1* mutation on the UPS, we evaluated the stability of three model substrates of the ubiquitin–proteasome pathway, namely, Ala-βgal, Arg-βgal, and Ub-Pro-βgal (Bachmair *et al.*, 1986). Whereas Ala-βgal is stable, Arg-βgal, and Ub-Pro-βgal are short-lived substrates of the N-end rule- and Ub-fusion degradation (UFD) pathway, respectively. Wild-type and *rpn5-1* mutant cells, transformed with plasmids expressing one of these substrates under a galactose inducible promoter were cultured at either 25 or 37°C. After 3 h, galactose was added to the culture to induce the production of the substrates, and cells were incubated for further 4 h. Total extract was prepared from each culture, and steady-state levels of the substrates were estimated by β-galactosidase assay. Compared with the wild-type cells, *rpn5-1* cells maintained the normally short-lived Arg-βgal and Ub-Pro-βgal at a higher level, especially at 37°C, indicating that the *rpn5-1* mutation caused a defect in the UPS at the restrictive temperature (Figure 1C).

Assembly of the Lid in rpn5-1 Mutants

In a previous report on a Δ*rpn5* mutant in fission yeast, the state of assembly of each substructure of the 26S proteasome was ambiguous, because Rpn10p that is not stably associated with the base or the lid was used for the affinity purification of proteasomes (Yen *et al.*, 2003a). To examine the assembly of the 26S proteasome in the *rpn5-1* mutant, we compared the gel filtration profile of proteasomes in wild-type and *rpn5-1* extracts. Wild-type and *rpn5-1* cells were cultured for 7 h at 37°C in YPDAU, and total lysates were prepared in the presence of ATP and $MgCl_2$. Extract equivalent to 5 mg of protein was resolved on a Superose 6 gel filtration column, and the eluate was collected into 500 μl of sequential fractions. Relevant fractions (16~32) were subjected to peptidase activity measurement by using succinyl-leucyl-leucyl-valyl-tyrosyl-methycoumaryl-7-amide (Suc-LLVY-MCA), a fluorogenic peptide substrate. In the wild-type sample, the most enzymatically active fraction was at 22, showing this fraction to be the peak fraction of the 26S holoenzyme (Figure 2A, top).

In contrast, in gel filtration of extract prepared from 37°C-grown *rpn5-1* cells, the peak at fraction 22 has almost vanished, suggesting that the assembly of the 26S proteasome is disturbed. On SDS treatment, which activates free CPs, a high enzyme activity occurred at fractions 26 and 27, indicating that there is a large pool of free CPs in *rpn5-1* cells grown at 37°C (Figure 2A, bottom). There was also a small peak in fraction 23, the identity of which will be discussed later. *rpn5-1* cells cultured at 25°C had almost the same profile as the wild-type, except that the peak of enzyme activity at fraction 26 was higher than that in the wild-type sample (Figure 2A, middle).

Fractions were then subjected to Western blotting by using antibodies against proteasome components. CP signals were detected around fraction 22 in the wild type sample, whereas they were detected around fraction 26 in the sample derived from *rpn5-1* cells grown at 37°C, in accordance with the result of activity measurement (Figure 2B, top and bottom). Interestingly, all lid components of *rpn5-1* cells grown at 37°C, but not at 25°C, were detected in low-molecular-mass fractions (Figure 2B, middle and bottom). To investigate whether they are monomers or forming a complex, we further resolved fractions 32 and 34 by Superdex 200, and fractions were subjected to Western blotting (Figure 2C). Comparison with marker proteins indicated that at least Rpn5p (52 kDa), Rpn8p (38 kDa), and Rpn9p (46 kDa) existed in a free form. Rpn7p (49 kDa) was found to move slower than expected from its molecular mass.

To see whether Rpn7p forms a stable complex with any other components in *rpn5-1* cells, we generated *rpn7::RPN7-3xFLAG* strains with or without the *rpn5-1* mutation and performed affinity purification. *RPN7-3xFLAG RPN5* and *RPN7-3xFLAG rpn5-1* strains were cultured at either 25 or 37°C for 7 h and proteasomes were affinity purified by anti-FLAG antibody immobilized on agarose from total lysates. Purified proteasomes were resolved by SDS-PAGE and stained with Coomassie brilliant blue (CBB), and the band patterns were compared with purified authentic proteasomes (Saeki *et al.*, 2005). All components of the 26S proteasome were copurified with Rpn7p-3xFLAG in wild-type cells and *rpn5-1* cells cultured at 25°C (Figure 2D, lanes 2 and 3; data for wild-type 25°C not shown). However, no protein was copurified with Rpn7p-3xFlag from *rpn5-1* cells cultured at 37°C. Because Rpn7p-3xFLAG was present in the total extract at both 37 and 25°C (Supplemental Figure 2), Rpn7p is probably not forming a soluble and stable complex with other components in *rpn5-1* cells under the restrictive conditions.

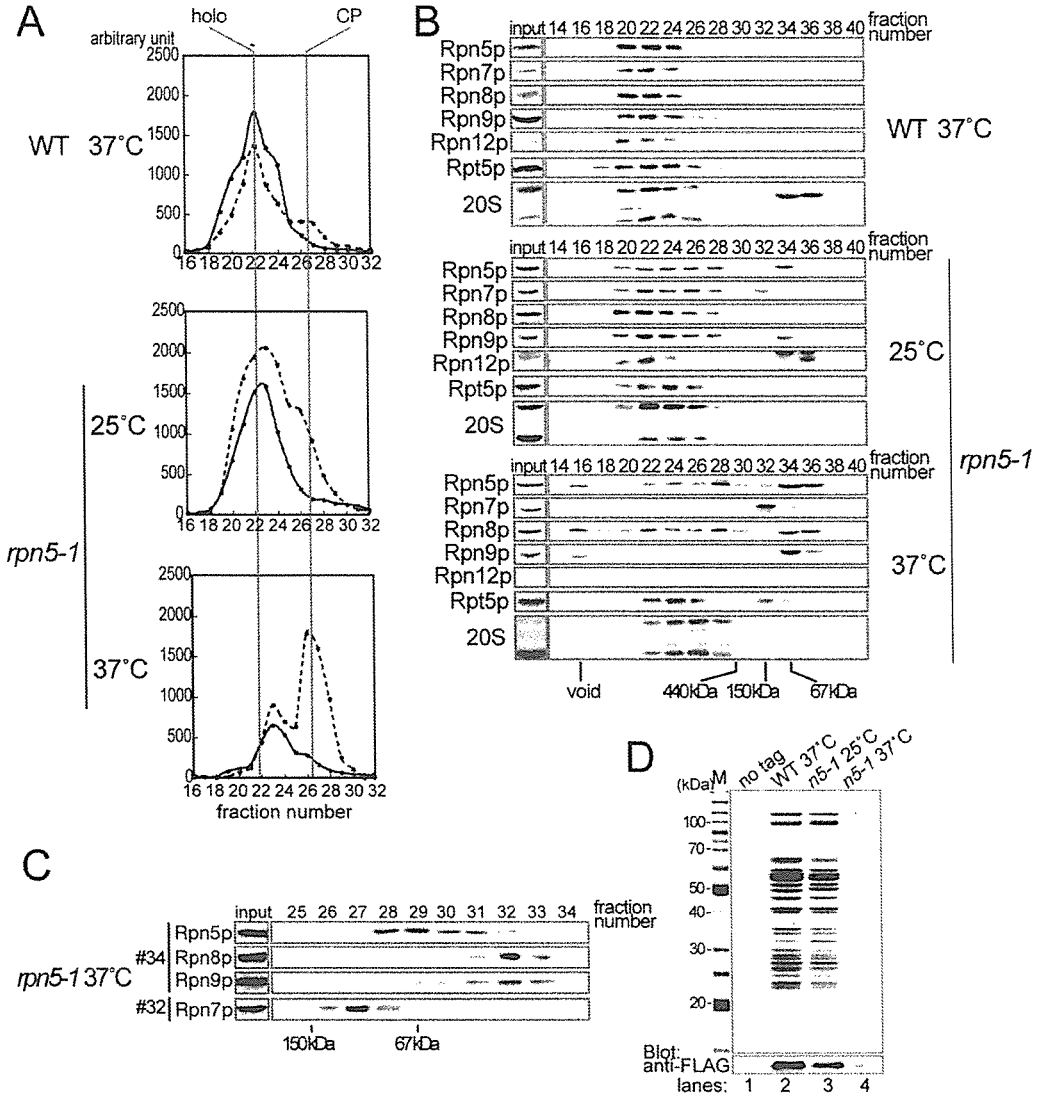

Figure 2. Lid formation in *rpn5-1* cells. Wild-type (W303-1A) and *rpn5-1* (YEK100) cells were cultured for 7 h at the indicated temperature, and total cell extracts were prepared by breaking the cells by glass-beads under the existence of ATP and $MgCl_2$. (A) Gel filtration. Peptidase activity toward the fluorogenic substrate Suc-LLVY-MCA was measured in relevant fractions (16–32). Positions of the 26S holoenzyme and the CP are indicated at the top of the graph. Solid line, without SDS; and dotted line, with 0.02% SDS. (B) Western blotting. Twenty microliters of each of the even numbered fractions was mixed with SDS-PAGE loading buffer and resolved by 12.5% SDS-PAGE, transferred to polyvinylidene difluoride membrane, and proteasome subunits were detected by Western blotting by using the indicated antibodies (Rpn5p, Rpn7p, Rpn8p, Rpn9p, and Rpn12p, lid; and Rpt5p, base) Positions of the void fraction and marker proteins (ferritin [440 kDa], aldolase [150 kDa], and bovine serum albumin [67 kDa]) are indicated at the bottom of the panels. (C) Second gel filtration. Fractions 32 and 34 in Superose 6 gel filtration of *rpn5-1* extracts (37°C) in A were subsequently resolved by a Superdex 200 gel filtration column. Five hundred microliters sequential fractions were collected, and relevant fractions were subjected to Western blotting as in B. Antibodies used are indicated on the left. Positions of marker proteins (aldolase [150 kDa] and bovine serum albumin [67 kDa]) are indicated on the bottom of the panels. (D) Wild-type and *rpn5-1* strains expressing *RPN7-3xFLAG* (YEK221 and YEK225, respectively) along with the untagged wild-type strain (W303-1A) were cultured for 7 h at 25 or 37°C as indicated, and extract was prepared from each culture. Proteasomes were affinity purified using anti-FLAG agarose. Purified products were run on a 12.5% SDS-PAGE gel, and protein bands were stained with CBB (M, marker).

Base-CP Complexes in rpn5-1

The base and the CP of the extract prepared from *rpn5-1* cells incubated at 37°C seemed to comigrate (Figure 2B). Results of nondenaturing PAGE of total lysates of wild-type or *rpn5-1* cells grown at 37°C showed the existence of base-CP complexes, B1CP, and B2CP, in *rpn5-1* cells (Figure 3A). The peak of peptidase activity observed in fraction 23 in the *rpn5-1* sample grown at 37°C (Figure 2A, bottom) was likely due to these base–CP complexes. We next tried to affinity-purify these base–CP complexes by using CP- or base-tagged strains. However, as shown in Figure 3B, no base–CP complex was obtained from *rpn5-1* cells regardless of the tagged subunit used, suggesting that the base-CP interaction in *rpn5-1* cells is unstable.

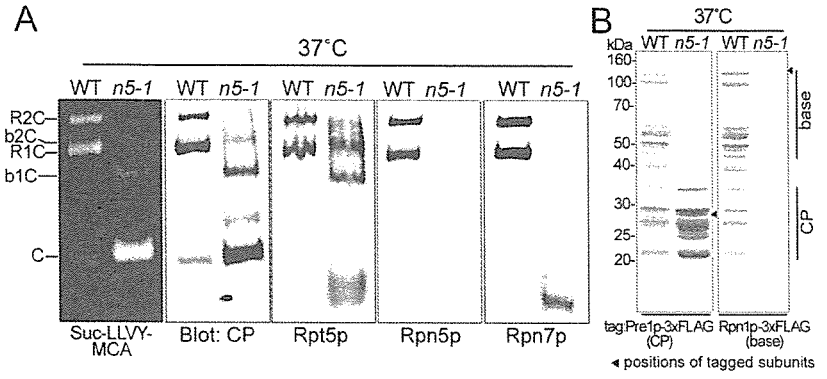

Figure 3. Proteasome species in wild-type extract and *rpn5-1* extract. (A) Extracts were prepared from wild-type (W303-1B) or *rpn5-1* (YEK101) cells incubated for 7 h at 37°C, and extract equivalent to 50 μg of protein was resolved by nondenaturing PAGE. Proteasomes were visualized by overlaying buffer containing 0.1 mM Suc-LLVY-MCA and 0.05% SDS on the gel (far left). The gels were subsequently subjected to Western blotting by using antibodies indicated on the bottom of the panels (Rpt5p, base; and Rpn5p and Rpn7p, lid). Bands corresponding to various proteasome species are indicated on the far left of the panels (R, RP; C, CP; and b, base). (B) Affinity purification of proteasomes from CP- and base-tagged stains. YYS37 (*PRE1-3xFLAG*) and YYS39 (*RPN1-3xFLAG*), YKN6 (*rpn5-1 PRE1-3xFLAG*) and YKN8 (*rpn5-1 RPN1-3xFLAG*) cells were cultured for 7 h at 37°C and proteasomes were affinity purified from 2 mg of total proteins using anti-FLAG agarose. The purified proteasomes were resolved on a 12.5% SDS-polyacrylamide gel and stained with CBB (left, CP tagged; and right, base tagged). Bands corresponding to the tagged components are indicated with solid arrowheads. The approximate migrating positions of the base and the CP components are indicated by bars on the right side of the panel.

Assembly of the Lid in a Base Mutant ΔN rpn2

In the previous section, we showed that the base was produced independently of the assembly of the lid. Next, we ask the following question: Are the lid and the base assembled independently to each other? To address this issue, we examined the status of lid assembly in a temperature-sensitive base mutant of *RPN2* termed *ΔN rpn2* (equivalent to *rpn2Δ* described by Yokota *et al.* 1996). *ΔN rpn2* is a mutant that carries an N-terminal truncated (Δ1-220aa) version of *RPN2* in a null *rpn2* strain. It stopped growth after 4–6 h at 37°C (data not shown). To see the assembly state in this mutant, total lysates were prepared from *ΔN rpn2* cells grown for 6 h at either 25 or 37°C, and 5 mg of total proteins was resolved on a Superose 6 gel filtration column.

The *ΔN rpn2* mutant was found to have a more severe defect in the structure of proteasomes than the *rpn5-1* mutant, because peptidase assays and Western blotting both showed reduced amount of the 26S holoenzyme even at the permissive temperature (Figure 4, A and B, left). The defects were strongly enhanced when cells were grown at the restrictive temperature. Peptidase activity measurement showed that in *ΔN rpn2* cells incubated at 37°C, the peak corresponding to the 26S proteasome was almost completely lost, and a single high peak of free CPs was detected at fraction no.26 (Figure 4A, right).

Western blotting of chromatographic fractions (Figure 4B, right) revealed that all lid components tested were detected in fraction no.28, which is comparable with the eluting position of a free lid (ca. 500 kDa). These results suggest that in *ΔN rpn2* under the restrictive condition, the lid exists in a free form, unbound to the base. Indeed, this was confirmed by native PAGE (Figure 4C) and affinity purification by using Rpn11p-3xFLAG (lid), by which a complete lid was affinity purified from *ΔN rpn2* cells (Figure 4D, lane 6). The incorporation of all of the nine lid components was verified by band comparison with a wild-type lid and liquid chromatography tandem mass spectrometry (Supplemental Figure 2). It was also shown that a ΔN Rpn2p-less base was formed in *ΔN rpn2* cells at the restrictive temperature (Figure 4D, lane 3). Together with the results of the *rpn5-1* extract, we conclude that the base formation and the lid formation can be independent of each other and are separable processes.

Localization of the Base and the CP in Lid Mutants

In yeast, the 26S proteasome is known to be highly enriched in the nucleus (Wilkinson *et al.*, 1998; Enenkel *et al.*, 1999). Biochemical analysis described above has shown that the lid formation was independent of the base formation. It is not known to date whether the assembly of the base and the lid into an RP is a prerequisite for their nuclear localization. To observe the localization of proteasomes in lid mutants, we generated GFP (Cormack *et al.*, 1996)-fused proteasomes, *PRE6-GFP* (CP), *RPN1-GFP* (base), and *RPN11-GFP* (lid) strains, in which one of the chromosomal *PRE6*, *RPN1*, and *RPN11* genes had been replaced with a C-terminally GFP-tagged gene, and the incorporation of the GFP-fused proteins into the proteasome were verified (Supplemental Figure 3).

Rpn1p-GFP and Pre6p-GFP showed strong nuclear localization in wild-type cells regardless of the incubating temperature (Figure 5A, left; data for 25°C not shown) as reported previously (Enenkel *et al.*, 1999; Wendler *et al.*, 2004). The localization was also examined in two lid mutants, *rpn5-1* and *rpn7-3*, in which the base was not associated with the lid under restrictive conditions. Both base and CP signals were observed in the nucleus regardless of the cultivation conditions (Figure 5A, middle and right), indicating that the *rpn5-1* and *rpn7-3* mutations that perturb the interaction between the lid and the base do not affect the nuclear localization of the base and the CP and that the nuclear localization of the base and the CP is independent of the binding of the lid to the base.

FRAP Experiments

One concern was that the base and CP signals detected at the restrictive temperature might be those of the remaining proteins synthesized and imported under the permissive temperature. To test this possibility, we observed the FRAP, by bleaching the nuclear region with intense laser and observing the recovery of fluorescence after 120 min.

We first carried out an experiment using a wild-type strain producing Rpn1p-GFP instead of Rpn1p. The GFP signals indeed vanished after photobleaching the region of the nucleus (Figure 5B, left and middle). When observed at 120 min after photobleaching, the GFP fluorescence occurred in the nucleus again, proving that nuclear import of the base has occurred (Figure 5B, right). Next, the recovery from photobleaching in *rpn7-3* cells was similarly examined using

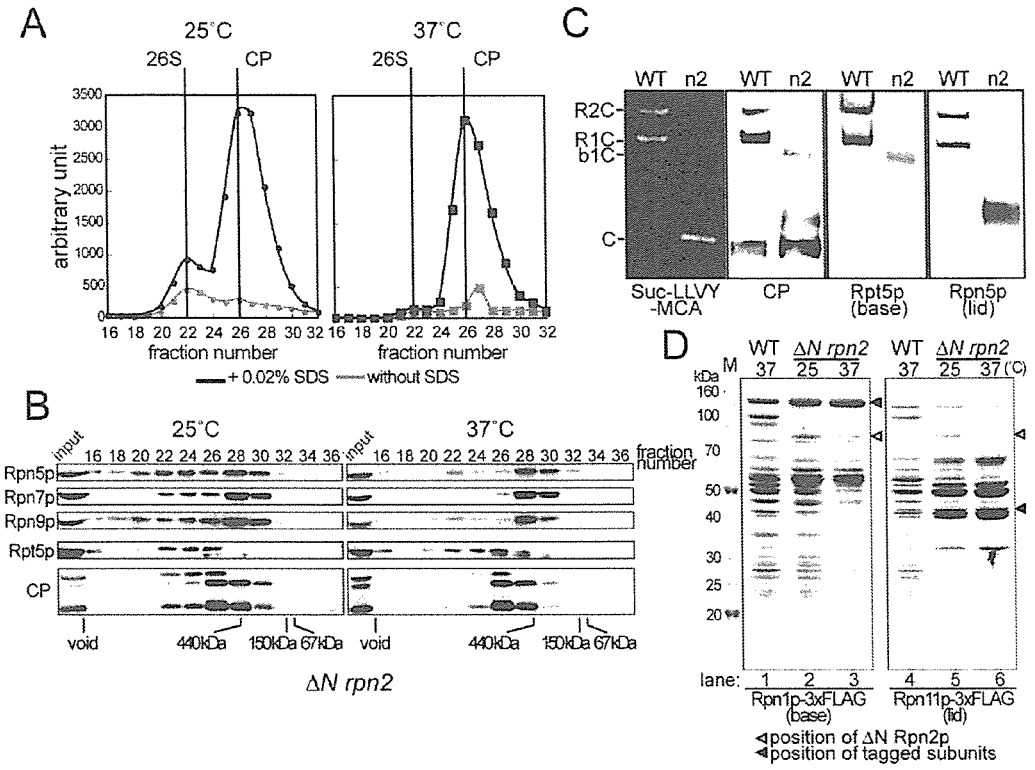

Figure 4. Lid formation does not depend on the binding of the lid to the base. (A) Extract of Δ*N rpn2* (YAT2433) cells cultured for 6 h at 25 or 37°C was resolved on a Superose 6 column, and peptidase activity was measured as described in Figure 2A. Positions of the 26S holoenzyme and the CP are indicated at the top of the graph (black lines, with 0.02% SDS; and gray lines, without SDS). (B) Fractions were subjected to Western blotting as described in Figure 2B. Antibodies used are indicated on the left of the panel (Rpn5p, Rpn7p, and Rpn9p, lid; and Rpt5, base). Positions of the void fraction and marker proteins (ferritin [440 kDa], aldolase [150 kDa], and bovine serum albumin [67 kDa]) are indicated at the bottom of the panels. Note that all lid components examined comigrated. (C) Wild-type (W303-1A) or Δ*N rpn2* (YAT2433) cells were cultured for 6 h at 37°C, and extract was prepared as described above. Extract equivalent to 50 μg of protein was resolved by nondenaturing PAGE. Proteasomes were visualized by overlaying buffer containing 0.1 mM Suc-LLVY-MCA and 0.05% SDS on the gels (far left panel). The same gels were subsequently subjected to Western blotting by using antibodies indicated on the bottom of the panels (Rpt5p, base; and Rpn5p, lid). Bands corresponding to various proteasome species are indicated on the far left of the panels (R, RP; C, CP; and b, base). (D) Affinity purification of proteasomes from base- and lid-tagged strains YYS39 (*RPN1-3xFLAG*), YYS40 (*RPN11-3xFLAG*), YEK234 (Δ*N rpn2 RPN1-3xFLAG*), and YAT3507 (Δ*N rpn2 RPN11-3xFLAG*) cells were cultured for 6 h at 25 or 37°C as indicated, and proteasomes were affinity-purified using anti-FLAG agarose. The purified proteasomes were resolved on a 12.5% SDS-polyacrylamide gel and stained with CBB (left, base tagged; and right, lid tagged). Protein bands were cut out and identified by mass spectrometry (see Supplemental Figure 2). The approximate migrating positions of base and lid components are indicated on the right of the panel (solid arrowhead, tagged component; open arrowhead, ΔN Rpn2p; and M, marker).

rpn7-3 strains expressing *RPN1-YGFP* and *PRE6-YGFP*. Cells were held under the restrictive condition by keeping the glass slides at 37°C by using a stage heater. In *rpn7-3* cells, recovery of both base and CP signals were observed even at the restrictive temperature (Figure 5, C and D). The fluorescence intensity in the nucleus was quantified and the degree of fluorescence recovery in *rpn7-3* cells was found to be comparable with that in the wild-type cells (Figure 5, C and D).

Localization of the Free Lid in ΔN rpn2 Cells

One of the striking features of the Δ*N rpn2* mutant is that its lid exists as a free complex. Because in no known mutant was the lid separated from the base in vivo, it has been difficult to examine whether the lid and the base could be imported into the nucleus independent of each other. We used the Δ*N rpn2* strain to observe the localization of the free lid along with the base by creating its *RPN11-GFP* (lid) or *RPN1-GFP* (base) derivative (Figure 6). Surprisingly, not only the base but also the lid was localized in the nucleus even at 37°C, suggesting that the import of the lid and the base does occur independently. It was verified by gel filtration (Figure 6B) and subsequent immunoprecipitaiton (Figure 6C) that the GFP signals corresponded to the respective complexes. The import of the lid into the nucleus under the restrictive condition was further corroborated by performing FRAP experiments (Figure 6D).

Localization of lid$^{rpn7\text{-}3}$ in rpn7-3 Cells

In the previously characterized *rpn7-3* mutant, it was shown that five of the nine lid components formed a subcomplex termed lid$^{rpn7\text{-}3}$ (Isono *et al.*, 2004). To see whether this partially assembled lid$^{rpn7\text{-}3}$ could be imported into the nucleus, we attempted to analyze the localization of lid$^{rpn7\text{-}3}$ in the *RPN11p-GFP rpn7-3* strain. However, because Rpn11p-GFP was not incorporated into lid$^{rpn7\text{-}3}$ at the restrictive temperature (data not shown), we observed its localization by using the indirect immunofluorescence method. *RPN11-3xFLAG* wild-type and *RPN11-3xFLAG rpn7-3* cells were

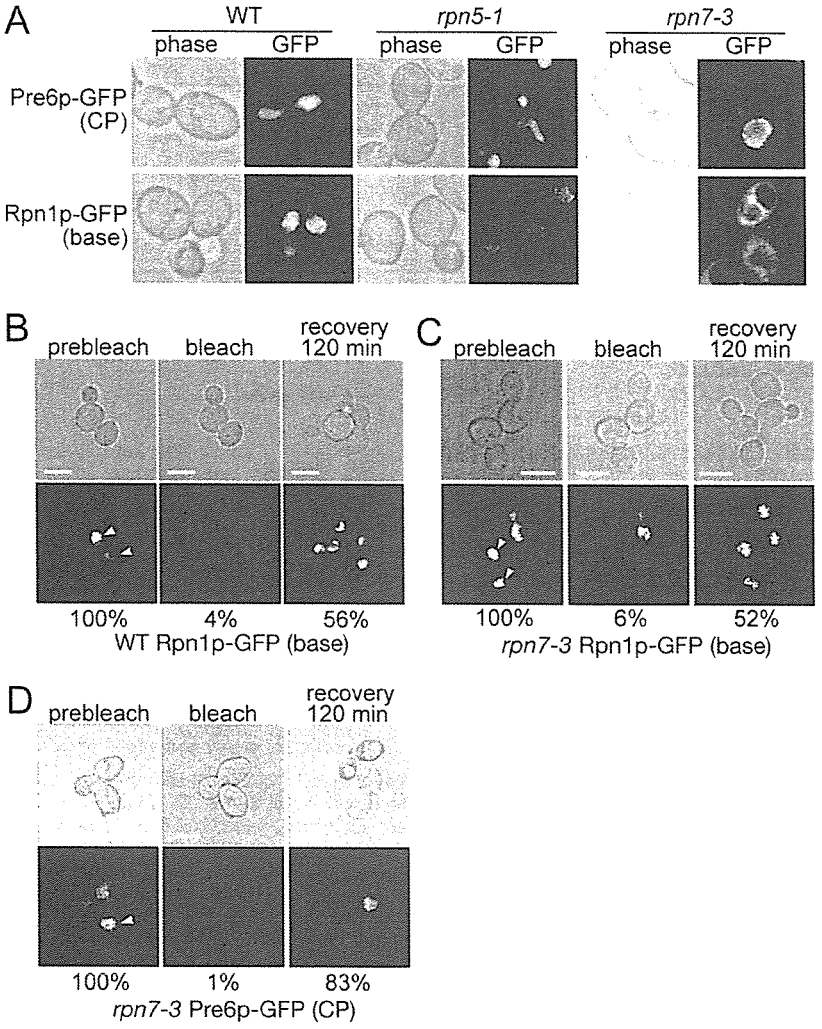

Figure 5. The base and the CP are localized in the nucleus in lid mutants even at the restrictive temperature. (A) Wild-type, *rpn5-1* and *rpn7-3* cells producing Pre6p-GFP (CP) or Rpn1p-GFP (base) instead of the authentic Pre6p and Rpn1p, respectively, were cultured for 7 h at 37°C and photographed under a confocal microscope. Strains used were *PRE6-GFP* (CP), wild type (YEK79), *rpn5-1* (YKN18), *rpn7-3* (YEK211), and *RPN1-GFP* (base) wild type (YEK147), *rpn5-1* (YKN16), *rpn7-3* (YEK213). (B–D) The base and the CP are imported into the nucleus after shift to the restrictive temperature. Rpn1p-GFP (base) producing wild-type (YEK147) and Rpn1p-GFP or Pre6p-GFP (CP) producing *rpn7-3* (YEK213 and YEK211, respectively) cells were cultured for 6 h at 37°C and embedded in agarose as described in *Materials and Methods*. GFP signals in the nucleus (prebleach, left) were photobleached with intense laser (bleach, middle), and FRAP was observed and photographed after 120 min (recovery, right). The stage was kept at 37°C throughout the experiment. Fluorescence intensity ([/mm^2] − background [/mm^2]) was quantified and shown as a relative value to the prebleach intensity at the bottom of each panel. The mean value of two independent experiments is shown. Bar; 5 μm.

cultured for 7 h at 37°C, fixed, and stained. In wild-type cells and *rpn7-3* cells cultured at 25°C, the signal corresponding to the 26S proteasome was clearly nuclear localized, and strong signals at the nuclear periphery was observed (Figure 7A, second and third panels from the top; data for 25°C wild-type samples not shown). On the contrary, in *rpn7-3* cells cultured at 37°C, the nuclear localization was not seen, and signals of DAPI-stained DNA did not merge with the FLAG signals any more (Figure 7A, lowermost panel), showing that the lid$^{rpn7\text{-}3}$ was not localized in the nucleus.

To confirm this observation, immunostaining was also performed using an antibody against Rpn5p, one of the components of lid$^{rpn7\text{-}3}$. Again, the nuclear localization seen in wild type cells could not be observed in the *rpn7-3* cells, in which signals of Rpn5p were detected dispersed in the cytosol (Figure 7B). This result suggests that the lid is built up in the cytosol and then imported into the nucleus to be assembled into the 26S complex, although we cannot exclude the possibility that the lid$^{rpn7\text{-}3}$ is reexported to the cytosol after carried into the nucleus. The structure of the nucleus itself was not damaged in *rpn7-3* cells under the restrictive condition, which was verified by the normal localization of mRFP (Campbell *et al.*, 2002) fused Nup53p, a component of the nuclear pore complex, in wild-type and also in *rpn7-3* cells at 37°C (Figure 7C).

From the above-mentioned results, we anticipated that the components not included in the lid$^{rpn7\text{-}3}$, namely, Rpn3p, Rpn7p, Rpn12p, and Rpn15p, might be responsible for the import of the lid. To test this possibility, we expressed one of the GFP-fused constructs of *RPN3*, *RPN7*, *RPN12*, or *RPN15* under their native promoters in *rpn5-1* cells. The cells were cultured for 7 h at 37°C and GFP signals were observed under a confocal microscope (Figure 7D). Rpn3p, Rpn7p, and Rpn12p showed nuclear localization, whereas Rpn15p did not, showing that Rpn3p, Rpn7p, and Rpn12p can be localized in the nucleus as monomers under these conditions.

The Nuclear Import of the Lid Does Not Depend on Srp1p

Srp1p, karyopherin α, was reported to be involved in the import of proteasomes into the nucleus (Tabb *et al.*, 2000; Lehmann *et al.*, 2002; Wendler *et al.*, 2004). In accordance with previous reports, in a temperature-sensitive mutant of *SRP1* termed *srp1-49*, Rpn11p-GFP (lid) and Rpn1p-GFP (base) were delocalized (Supplemental Figure 4). However, because no method has been available to form the lid and

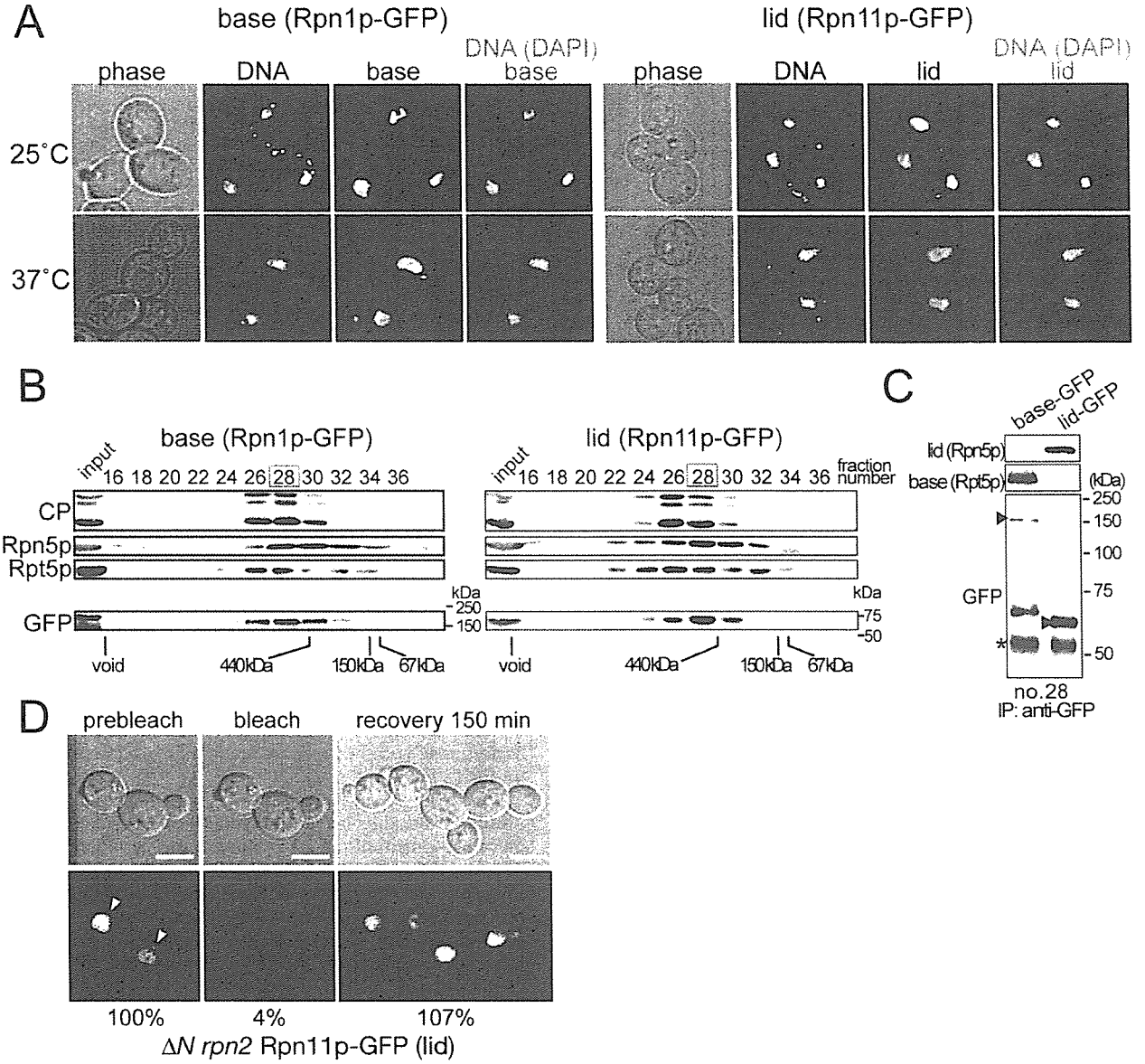

Figure 6. The nuclear import of the base and the lid are independent of each other. (A) Δ*N rpn2* cells producing Rpn1p-GFP (base, YEK235) or Rpn11p-GFP (lid, YEK236) instead of the authentic Rpn1p or Rpn11p, respectively, were cultured for 6 h at either 25 or 37°C and photographed under a confocal microscope. DNA was stained with Hoechst 33342. (B) Total proteins were extracted from the cells cultured at 37°C as described in A and subjected to gel filtration by using a Superose 6 column. Fractions were subsequently subjected to Western blotting by using the antibodies indicated on the left of the panels. (Rpn5p; lid, Rpt5p; base) Positions of the void fraction and marker proteins (ferritin [440 kDa], aldolase [150 kDa], and bovine serum albumin [67 kDa]) are indicated at the bottom of the panels. For the GFP blot, positions of molecular mass markers are shown on the right of each of the panels. (C) Immunoprecipitation was performed against fraction 28 in B by using anti-GFP antibody and analyzed by Western blotting by using anti-Rpn5p (lid), anti-Rpt5p (base), and anti-GFP antibodies. Asterisks indicate nonspecific bands. Arrowheads indicate the GFP-fused components. (D) *RPN11-GFP*–expressing Δ*N rpn2* (YEK256) cells were cultured for 6 h at 37°C, and FRAP experiments were performed as in Figure 5, except that the recovery was observed after 150 min. Fluorescence intensity ([/mm^2] − background [/mm^2]) was quantified and shown as relative values to the prebleach intensity at the bottom of each panel. The mean value of two independent experiments is shown. Arrowheads indicate the cell that was photobleached. Bar; 5 μm.

the base separately in vivo, it had been impossible to examine whether their nuclear import would be dependent on Srp1p.

To address this issue, we took advantage of the Δ*N rpn2* mutant, in which the lid exists as a free complex at the restrictive temperature. Either *RPN7-GFP* or *RPN1-GFP* was introduced into the Δ*N rpn2 srp1-49* double mutant to replace each of the authentic genes. Cells were cultured for 8 h at 37°C and observed under a confocal microscope. Although the base lost its strong nuclear localization seen at 25°C, and a part of the signals was dispersed in the cytosol, the lid signals remained strongly in the nucleus at 37°C (Figure 8A), which was corroborated by the quantification of the fluorescence signals (Figure 8B). These results suggest

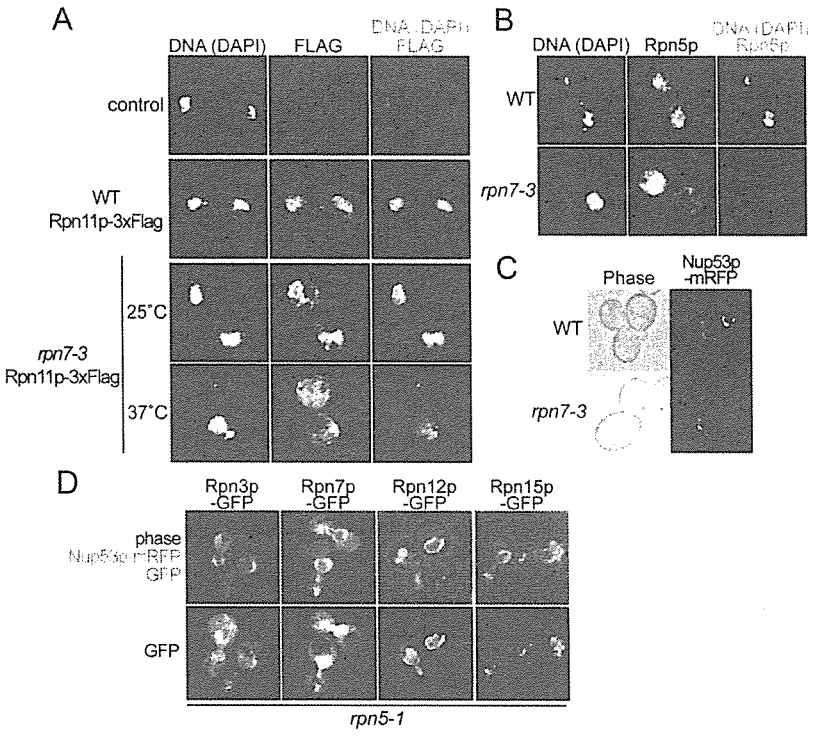

Figure 7. Localization of the partially assembled lid$^{rpn7\text{-}3}$. (A) *RPN11-3xFLAG* (YYS40) and *rpn7-3 RPN11-3xFLAG* (YEK29) cells, along with untagged wild-type (W303-1A) cells, were cultured for 6 h at 25 or 37°C as indicated, and localization of lid$^{rpn7\text{-}3}$ was detected by the indirect immunofluorescence method by using anti-FLAG M2 antibody. Photographs were taken under a confocal microscope. DNA was stained with DAPI. (B) Wild-type (W303-1B) and *rpn7-3* (YEK6) cells were incubated for 6 h at 37°C, and localization of Rpn5p was detected as described in A by the indirect immunofluorescence method except that an anti-Rpn5p antibody was used. DNA was stained with DAPI. (C) The nuclear envelope is normal in *rpn7-3* cells under the restrictive condition. Nup53p-mRFP (pEK285) was produced in wild-type (W303-1A) and *rpn7-3* (YEK6) cells cultured at the same condition as described in B and photographed under a confocal microscope. (D) Localization of Rpn3p-GFP (pEK297), Rpn7p-GFP (pEK298), Rpn12p-GFP (pEK299), or Rpn15p-GFP (pEK300) in *rpn5-1* (YEK100) cells. Cells were cultured for 8 h at 37°C, and GFP signals were photographed under a confocal microscope. Nup53p-mRFP was used as a marker for the nuclear envelope.

that the nuclear import of the base is dependent on Srp1p, whereas that of the lid does not.

DISCUSSION

The *RPN5* gene, originally named *n*on-*A*TPase subunit 5 (*NAS5*), is an essential gene in *S. cerevisiae*, in contrast to *Schizosaccharomyces pombe*, and is a homologue of human p55 (Finley *et al.*, 1998). In this study, we have shown that in *rpn5-1* cells, not even a partially assembled subcomplex of the lid was detected at the restrictive temperature (Figure 2, B–D). This result, together with our previous reports, indicates that the mutation in Rpn5p inhibits the complex formation of the lid, and thus Rpn5p is a key component in the core formation of the lid. A very recently published report has shown the interaction between subunits of the RP by tandem MS analysis (Sharon *et al.*, 2006). Using this novel approach, it was demonstrated that Rpn5p, Rpn8p, Rpn9p, and Rpn11p is forming a stable soluble subcomplex and a subunit interaction map was proposed, which is in good accordance with our results that Rpn5p is a core component in lid formation.

Interestingly, the addition of a 3xFLAG tag at the C terminus to another lid component Rpn11p rescued the temperature-sensitivity of *rpn5-1* and at the same time its defect in assembling the 26S proteasome (Supplemental Figure 6). Probably, the C terminus of Rpn11p is located near to the C terminus of Rpn5p so that its extension suppresses the structural alternation of the proteasome caused by the incorporation of the truncated Rpn5-1p. Because the structural recovery of the 26S proteasome led to a complete growth recovery at the restrictive temperature, the *rpn5-1* mutation was probably causing purely structural defects.

The fact that the base-CP interaction in mutant cells is unstable indicates the possibility that the lid functions to strengthen the base-CP binding by allosterically affecting the base-CP interface. This result is in contrast to a previous report in which a base-CP complex was purified from a mutant of *RPN11* termed *mpr1–1* in the absence of the lid

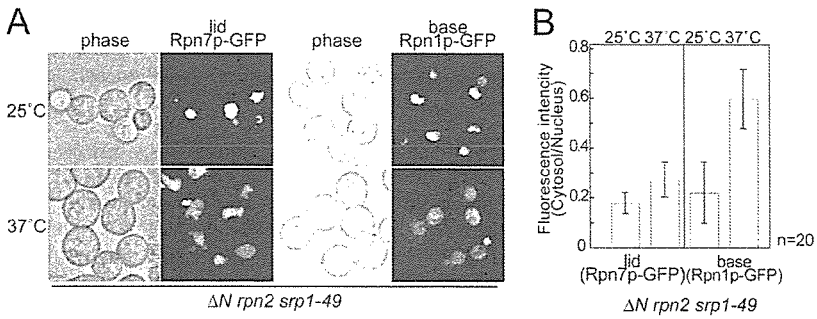

Figure 8. Nuclear localization of the base, but not the lid, is affected by *srp1-49*. (A) Δ*N rpn2 srp1-49* cells expressing Rpn7p-GFP or Rpn1p-GFP (YEK247 and YEK258, respectively) were cultured for 8 h at either 25 or 37°C, and localization of the GFP-fused components was observed under a confocal microscope. (B) Signals of A were quantified (fluorescence intensity per area) using the IPLab software, and ratio of the nuclear and cytosolic signals is shown. Error bars represent SD (n = 20).

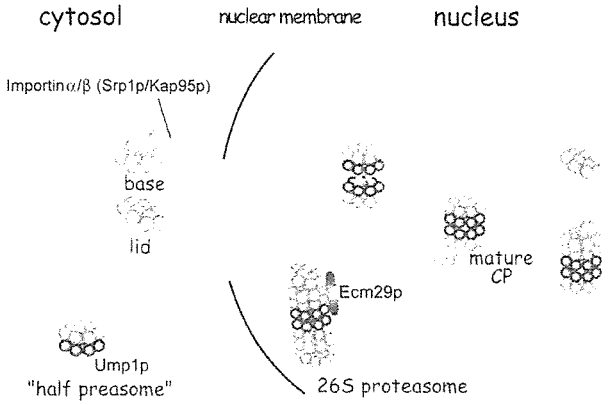

Figure 9. Model for the assembling process of the 26S proteasome in budding yeast. The base and the lid are made in the cytosol and are imported into the nucleus independently. On the dimerization of half-proteasomes into a mature CP, the base binds the CP. The immediate binding of the lid to the base–CP complex stabilizes the whole complex. Additional interacting proteins are bound to the 26S proteasome.

(Verma *et al.*, 2002). We have no explanation for this discrepancy at present.

In fission yeast, it was proposed that SpRpn5, together with the human breast cancer related gene Int6/Yin6, serves for the nuclear localization of the lid (Yen *et al.*, 2003b), although our results showed that the lid$^{rpn7\text{-}3}$ containing Rpn5p was not localized in the nucleus (Figure 7, A and B). One explanation of these seemingly controversial results may be that there is no Int6/Yin6 homologue in budding yeast and hence the Int6/Yin6 associated function of Rpn5p is not conserved in the two yeast species.

The CP and an interacting ATPase exist already in prokaryotic organisms. Given that the lid shares its origin with COP9/signalosme and eIF3, both of which are functioning as a single complex, it is reasonable that the formation and the nuclear localization of the base and the lid are independent to each other. However, although the base is imported into the nucleus via the Srp1p-dependent importin α/β pathway, the lid seems to be carried into the nucleus via another system that is independent of Srp1p (Figure 8, A and B). As for the base, two of the base components, Rpn2p and Rpt2p, were shown to possess functional nuclear localization signal (NLS) sequences, and because the simultaneous deletion of these sequences is lethal, it was suggested that the nuclear import of the base probably depends on its own NLS(s) (Wendler *et al.*, 2004). No component of the lid was yet proved to be responsible for the nuclear import of the lid. Our results suggest that Rpn3p, Rpn7p, and Rpn12, each of which is localized into nucleus by itself, may serve for the nuclear import of the lid (Figure 7D).

We have shown in this study that the lid, a substructure of the 26S proteasome, can be formed and imported into the nucleus independently of the other subcomplexes of the 26S proteasome. Together with the result that a base–CP complex is formed in the analyzed lid mutants, we propose the following scenario of the assembling pathway of the 26S proteasome (Figure 9). The half-proteasome as well as base and the lid are formed independently in the cytosol, and they are imported into the nucleus. Then, the base binds the mature CP, and finally the lid binds the base–CP complex to form a mature 26S proteasome. In the course of the formation of the lid, Rpn5p, together with its interacting components forms the core of the lid, into which Rpn6p then the rest of the components are sequentially incorporated to become a complete lid. It should be noted that the scenario of the assembly pathway described above had been drawn using mutants, and there might be a different pathway in wild-type cells. In wild-type cells, the assembly processes are probably too rapid to be detected biochemically, because the apparent intermediates of the 26S proteasome such as the base–CP complex, lid$^{rpn6\text{-}1}$ and lid$^{rpn7\text{-}3}$ existed in lid mutants under the restrictive condition (Isono *et al.*, 2004, 2005) cannot be detected.

This consideration casts another question as to whether there are any factors that facilitate or regulate the interaction between the base, lid and CP. It should be noted that a recent report with mammalian cells has shown that a protein interacting with the ATPase subunits of the base, named PAAF1, inhibits the binding of the RP and the CP (Park *et al.*, 2005). Whether external factors are involved in the formation of the lid and the base is also a question that remains to be answered.

ACKNOWLEDGMENTS

We thank Dr. Daniel Finley (Harvard University, Boston, MA) for the anti-Rpn8p antibody, Dr. Jussi Jantti (University of Helsinki, Helsinki, Finland) for the anti-Sem1p (Rpn15p) antibody, and Dr. Roger Tsien (University of California, San Diego, San Diego, CA) for the mRFP1 plasmid. We are grateful to Dr. Cordula Enenkel (Humboldt University, Berlin, Germany) for valuable suggestions and advice, Drs. Satoshi Yoshida (Harvard University, Boston, MA) and Takashi Itoh (RIKEN, Saitama, Japan) for technical advice, and the members of the Laboratory of Genetics for discussions and comments. Thanks are also due to Drs. Yoshibumi Komeda and Ichiro Terashima (University of Tokyo, Tokyo, Japan) for generously letting us use the laboratory space and to Naoko Saito for earlier contribution to this work. This work was supported by a grant-in-aid for scientific research from the Ministry of Education, Culture, Sports, Science, and Technology (to A.T.) and by a grant-in-aid from the Japan Society for Promotion of Young Scientists (to E.I.).

REFERENCES

Bachmair, A., Finley, D., and Varshavsky, A. (1986). In vivo half-life of a protein is a function of its amino-terminal residue. Science *234*, 179–186.

Burk, D., Dawson, D., and Stearns, T. (2000). Methods in Yeast Genetics. Cold Spring Harbor, NY: Cold Spring Harbor Laboratory Press.

Cadwell, R. C., and Joyce, G. F. (1992). Randomization of genes by PCR mutagenesis. PCR Methods Appl. *2*, 28–33.

Campbell, R. E., Tour, O., Palmer, A. E., Steinbach, P. A., Baird, G. S., Zacharias, D. A., and Tsien, R. Y. (2002). A monomeric red fluorescent protein. Proc. Natl. Acad. Sci. USA *99*, 7877–7882.

Chen, P., and Hochstrasser, M. (1996). Autocatalytic subunit processing couples active site formation in the 20S proteasome to completion of assembly. Cell *86*, 961–972.

Cope, G. A., Suh, G. S., Aravind, L., Schwarz, S. E., Zipursky, S. L., Koonin, E. V., and Deshaies, R. J. (2002). Role of predicted metalloprotease motif of Jab1/Csn5 in cleavage of Nedd8 from Cul1. Science *298*, 608–611.

Cormack, B. P., Valdivia, R. H., and Falkow, S. (1996). FACS-optimized mutants of the green fluorescent protein (GFP). Gene *173*, 33–38.

Elsasser, S., Chandler-Militello, D., Muller, B., Hanna, J., and Finley, D. (2004). Rad23 and Rpn10 serve as alternative ubiquitin receptors for the proteasome. J. Biol. Chem. *279*, 26817–26822.

Enenkel, C., Lehmann, A., and Kloetzel, P. M. (1999). GFP-labelling of 26S proteasomes in living yeast: insight into proteasomal functions at the nuclear envelope/rough ER. Mol. Biol. Rep. *26*, 131–135.

Fehlker, M., Wendler, P., Lehmann, A., and Enenkel, C. (2003). Blm3 is part of nascent proteasomes and is involved in a late stage of nuclear proteasome assembly. EMBO Rep. *4*, 959–963.

Finley, D., *et al.* (1998). Unified nomenclature for subunits of the *Saccharomyces cerevisiae* proteasome regulatory particle. Trends Biochem. Sci. *23*, 244–245.

Fu, H., Reis, N., Lee, Y., Glickman, M. H., and Vierstra, R. D. (2001). Subunit interaction maps for the regulatory particle of the 26S proteasome and the COP9 signalosome. EMBO J. *20*, 7096–7107.

Funakoshi, M., Li, X., Velichutina, I., Hochstrasser, M., and Kobayashi, H. (2004). Sem1, the yeast ortholog of a human BRCA2-binding protein, is a component of the proteasome regulatory particle that enhances proteasome stability. J. Cell Sci. *117*, 6447–6454.

Glickman, M. H., Rubin, D. M., Coux, O., Wefes, I., Pfeifer, G., Cjeka, Z., Baumeister, W., Fried, V. A., and Finley, D. (1998a). A subcomplex of the proteasome regulatory particle required for ubiquitin-conjugate degradation and related to the COP9-signalosome and eIF3. Cell *94*, 615–623.

Glickman, M. H., Rubin, D. M., Fried, V. A., and Finley, D. (1998b). The regulatory particle of the *Saccharomyces cerevisiae* proteasome. Mol. Cell Biol. *18*, 3149–3162.

Guterman, A., and Glickman, M. H. (2004). Complementary roles for Rpn11 and Ubp6 in deubiquitination and proteolysis by the proteasome. J. Biol. Chem. *279*, 1729–1738.

Hershko, A., and Ciechanover, A. (1998). The ubiquitin system. Annu. Rev. Biochem. *67*, 425–479.

Hirano, Y., Hendil, K. B., Yashiroda, H., Iemura, S., Nagane, R., Hioki, Y., Natsume, T., Tanaka, K., and Murata, S. (2005). A heterodimeric complex that promotes the assembly of mammalian 20S proteasomes. Nature *437*, 1381–1385.

Hoepfner, D., Brachat, A., and Philippsen, P. (2000). Time-lapse video microscopy analysis reveals astral microtubule detachment in the yeast spindle pole mutant cnm67. Mol. Biol. Cell *11*, 1197–1211.

Hofmann, K., and Bucher, P. (1998). The PCI domain: a common theme in three multiprotein complexes. Trends Biochem. Sci. *23*, 204–205.

Isono, E., Saeki, Y., Yokosawa, H., and Toh-e, A. (2004). Rpn7 Is required for the structural integrity of the 26 S proteasome of *Saccharomyces cerevisiae*. J. Biol. Chem. *279*, 27168–27176.

Isono, E., Saito, N., Kamata, N., Saeki, Y., and Toh, E. A. (2005). Functional analysis of Rpn6p, a lid component of the 26 S proteasome, using temperature-sensitive rpn6 mutants of the yeast *Saccharomyces cerevisiae*. J. Biol. Chem. *280*, 6537–6547.

Leggett, D. S., Hanna, J., Borodovsky, A., Crosas, B., Schmidt, M., Baker, R. T., Walz, T., Ploegh, H., and Finley, D. (2002). Multiple associated proteins regulate proteasome structure and function. Mol. Cell *10*, 495–507.

Lehmann, A., Janek, K., Braun, B., Kloetzel, P. M., and Enenkel, C. (2002). 20 S proteasomes are imported as precursor complexes into the nucleus of yeast. J. Mol. Biol. *317*, 401–413.

Maytal-Kivity, V., Reis, N., Hofmann, K., and Glickman, M. H. (2002). MPN+, a putative catalytic motif found in a subset of MPN domain proteins from eukaryotes and prokaryotes, is critical for Rpn11 function. BMC Biochem. *3*, 28.

Park, Y., Hwang, Y. P., Lee, J. S., Seo, S. H., Yoon, S. K., and Yoon, J. B. (2005). Proteasomal ATPase-associated factor 1 negatively regulates proteasome activity by interacting with proteasomal ATPases. Mol. Cell Biol. *25*, 3842–3853.

Ramos, P. C., Hockendorff, J., Johnson, E. S., Varshavsky, A., and Dohmen, R. J. (1998). Ump1p is required for proper maturation of the 20S proteasome and becomes its substrate upon completion of the assembly. Cell *92*, 489–499.

Saeki, Y., Isono, E., and Toh-e, A. (2005). Preparation of ubiquitinated substrates by the PY motif-insertion method for monitoring 26S proteasome activity. Methods Enzymol. *399*, 215–227.

Saeki, Y., Saitoh, A., Toh-e, A., and Yokosawa, H. (2002). Ubiquitin-like proteins and Rpn10 play cooperative roles in ubiquitin-dependent proteolysis. Biochem. Biophys. Res. Commun. *293*, 986–992.

Sasaki, T., Toh-e, A., and Kikuchi, Y. (2000). Yeast Krr1p physically and functionally interacts with a novel essential Kri1p, and both proteins are required for 40S ribosome biogenesis in the nucleolus. Mol. Cell. Biol. *20*, 7971–7979.

Schmidt, M., Haas, W., Crosas, B., Santamaria, P. G., Gygi, S. P., Walz, T., and Finley, D. (2005). The HEAT repeat protein Blm10 regulates the yeast proteasome by capping the core particle. Nat. Struct. Mol. Biol. *12*, 294–303.

Schwartz, A. L., and Ciechanover, A. (1999). The ubiquitin-proteasome pathway and pathogenesis of human diseases. Annu. Rev. Med. *50*, 57–74.

Sharon, M., Taverner, T., Ambroggio, X. I., Deshaies, R. J., and Robinson, C. V. (2006). Structural organization of the 19S proteasome lid: insights from MS of intact complexes. PLoS Biol. *4*.

Sherman, F., Fink, G. R., and Hicks, J. B. (1986). Methods in Yeast Genetics, Cold Spring Harbor, NY: Cold Spring Harbor Laboratory Press, 12–18.

Sikorski, R. S., and Hieter, P. (1989). A system of shuttle vectors and yeast host strains designed for efficient manipulation of DNA in *Saccharomyces cerevisiae*. Genetics *122*, 19–27.

Sone, T., Saeki, Y., Toh-e, A., and Yokosawa, H. (2004). Sem1p is a novel subunit of the 26 S proteasome from *Saccharomyces cerevisiae*. J. Biol. Chem. *279*, 28807–28816.

Tabb, M. M., Tongaonkar, P., Vu, L., and Nomura, M. (2000). Evidence for separable functions of Srp1p, the yeast homolog of importin alpha (Karyopherin alpha): role for Srp1p and Sts1p in protein degradation. Mol. Cell Biol. *20*, 6062–6073.

Takeda, K., and Yanagida, M. (2005). Regulation of nuclear proteasome by Rhp6/Ubc2 through ubiquitination and destruction of the sensor and anchor Cut8. Cell *122*, 393–405.

Tatebe, H., and Yanagida, M. (2000). Cut8, essential for anaphase, controls localization of 26S proteasome, facilitating destruction of cyclin and Cut2. Curr. Biol. *10*, 1329–1338.

Toh-e, A., and Oguchi, T. (2000). An improved integration replacement/disruption method for mutagenesis of yeast essential genes. Genes Genet. Syst. *75*, 33–39.

van Nocker, S., Sadis, S., Rubin, D. M., Glickman, M., Fu, H., Coux, O., Wefes, I., Finley, D., and Vierstra, R. D. (1996). The multiubiquitin-chain-binding protein Mcb1 is a component of the 26S proteasome in *Saccharomyces cerevisiae* and plays a nonessential, substrate-specific role in protein turnover. Mol. Cell Biol. *16*, 6020–6028.

Verma, R., Aravind, L., Oania, R., McDonald, W. H., Yates, J. R., 3rd, Koonin, E. V., and Deshaies, R. J. (2002). Role of Rpn11 metalloprotease in deubiquitination and degradation by the 26S proteasome. Science *298*, 611–615.

Wendler, P., Lehmann, A., Janek, K., Baumgart, S., and Enenkel, C. (2004). The bipartite nuclear localization sequence of Rpn2 is required for nuclear import of proteasomal base complexes via karyopherin $\alpha\beta$ and proteasome functions. J. Biol. Chem. *279*, 37751–37762.

Wilkinson, C. R., Wallace, M., Morphew, M., Perry, P., Allshire, R., Javerzat, J. P., McIntosh, J. R., and Gordon, C. (1998). Localization of the 26S proteasome during mitosis and meiosis in fission yeast. EMBO J. *17*, 6465–6476.

Yao, T., and Cohen, R. E. (2002). A cryptic protease couples deubiquitination and degradation by the proteasome. Nature *419*, 403–407.

Yen, H. C., Espiritu, C., and Chang, E. C. (2003a). Rpn5 is a conserved proteasome subunit and required for proper proteasome localization and assembly. J. Biol. Chem. *278*, 30669–30676.

Yen, H. C., Gordon, C., and Chang, E. C. (2003b). *Schizosaccharomyces pombe* Int6 and Ras homologs regulate cell division and mitotic fidelity via the proteasome. Cell *112*, 207–217.

Yokota, K., *et al.* (1996). CDNA cloning of p112, the largest regulatory subunit of the human 26s proteasome, and functional analysis of its yeast homologue, sen3p. Mol. Biol. Cell *7*, 853–870.